

PDA-86-FR-5333-00-06

THE APPLICATION OF CAST SiC/Al
TO ROTARY ENGINE COMPONENTS

SBIR PHASE I - FINAL REPORT

August 15, 1986

Contract No. NAS3-~~24847~~ 24847

H.M. Stoller
J.R. Carluccio
J.P. Norman

PDA Engineering
1560 Brookhollow Drive
Santa Ana, CA 92705

(NASA-CR-179610) THE APPLICATION OF CAST
SiC/Al TO ROTARY ENGINE COMPONENTS Final
Report (PDA Engineering) 101 p CSCL 21F

N90-13385

Unclass

63/07 0235020

NOTICE

The applications study conducted in this SBIR Phase I program considered only one SiC/Al material fabricated by Dural Aluminum Composites Corporation (DACC). Any materials deficiencies uncovered in this investigation are assumed to be associated with the relative state of materials development. The use of DACC's SiC/Al material in this investigation does not constitute an endorsement by PDA Engineering for other applications.

PRECEDING PAGE BLANK NOT FILMED

ORIGINAL PAGE
BLACK AND WHITE PHOTOGRAPH



Modeled by J. Bentley, PDA; Courtesy of John Deere

Figure 1. PATRAN Solid Representation of a Rotor

TABLE OF CONTENTS

<u>Section</u>	<u>Page</u>
1.0 INTRODUCTION, WORK STATEMENT, AND SUMMARY	1
1.1 Introduction	1
1.2 Phase I Statement of Work	6
1.3 Summary	9
2.0 TEST MATERIALS AND PHYSICAL CHARACTERIZATION	17
2.1 Test Materials	17
2.2 Physical Characterization	18
3.0 MECHANICAL PROPERTIES OF SiC/Al	25
3.1 Introduction	25
3.2 Hardness	25
3.3 High Temperature Strength and Stiffness Properties	27
3.4 Wear Resistance	30
3.5 Fatigue Resistance	32
4.0 THERMAL PROPERTIES OF SiC/Al	33
4.1 Thermal Conductivity	33
4.2 Thermal Expansion	34
5.0 COATINGS COMPATIBILITY	36
6.0 EVALUATION OF POSSIBLE COMPONENT APPLICATIONS	38
6.1 Trochoid Housing	38
6.2 End Housing	40
6.3 Seals - Apex, Corner and Side	40
6.4 Rotor	41
7.0 FEASIBILITY DESIGN STUDY - SiC/Al ROTOR	43
7.1 Overview	43
7.2 Finite Element Model	43
7.3 Analyses	43
7.3.1 Thermal Analyses	46
7.3.2 Static Analyses	46
7.3.3 Fatigue Analyses	50
8.0 CONCLUSIONS AND RECOMMENDATIONS	56
8.1 Conclusions	56
8.2 Recommendations	56
9.0 REFERENCES	58

TABLE OF CONTENTS (Continued)

<u>Appendices</u>	<u>Page</u>
A	Manufacturer's Mechanical Properties Data on A201-T6 60
B	High Temperature Modulus Data 63
C	Thermal Conductivity of 10 v/o and 20 v/o SiC/A201-T6 70
D	Thermal Expansion of 10 v/o and 20 v/o SiC/A201-T6 85

LIST OF FIGURES

<u>Figure</u>	<u>Page</u>
1	PATRAN Solid Representation of a Rotor iv
2	Cross-Sectional Representation of Rotary Engine Housing. 3
3	Representative Fabrication Techniques for Cast SiC/Al. 5
4	Billets of As-Received SiC/A201 17
5	Radiographs of 10 v/o Billets. 19
6	Radiographs of 20 v/o Billets. 20
7	Micrographs of High Density Inclusions in 20 v/o Billets 22
8	Micrographs of 10 v/o and 20 v/o Billets 23
9	Manufacturer's Hardness Data for A201-T6 26
10	Yield Strength of SiC/A201-T6 Alloy 28
11	Ultimate Strength of SiC/A201-T6 Alloy 29
12	Average Young's Modulus for SiC/A201-T6 31
13	Finite Element Model of NASA Rotor 44
14	Cyclic Stress Profile 44
15	A Comparison of Temperature Distributions in SiC/Al and Stainless Steel Rotors 47
16	A Comparison of Thermal Stresses in SiC/Al and Stainless Steel Rotors 48
17	Top Dead Center Applied Loads 49
18	A Comparison of Static Stress Levels (TDC Condition) in SiC/Al and Stainless Steel Rotors 51
19	A Comparison of Static Stress Levels (BDC Condition) in SiC/Al and Stainless Steel Rotors 52
20	A Comparison of Cyclic Stresses in SiC/Al and Stainless Steel Rotors 53

LIST OF TABLES

<u>Table</u>	<u>Page</u>
1	Hardness Values of A201-T6 Materials 26
2	Thermal Conductivity Measurements of SiC/Al. 33
3	Coefficient of Thermal Expansion Data 34
4	Comparison of CTEs - Materials of Interest 37
5	A Comparison of Mean and Amplitude Stresses - Shallow Pocket Rib 54

1.0 INTRODUCTION, WORK STATEMENT, SUMMARY

1.1 Introduction

Important developments have been occurring in metal matrix composites (MMC) technology which could be of major significance to the development of advanced rotary combustion engines. One of the most promising of these developments is silicon carbide reinforced-aluminum (SiC/Al) where whiskers, flakes, or particulates of silicon carbide are used as the reinforcing constituent for the aluminum alloy matrix of interest.

At the time of the SBIR Phase I proposal preparation [1], specific stiffness increases up to 70 percent [2] and specific strength increases up to 30 percent [3], relative to the properties of the aluminum alloy employed as the matrix material, had been reported. A major effect of the SiC reinforcement, where strength increases are obtained, is the retention of this strength increase and the stiffness increase to higher temperatures. These effects have the potential of increasing the operating temperature capability of aluminum on the order of one hundred degrees, Fahrenheit [3]. In addition to these potential high temperature strength and stiffness improvements, other reported property characteristics of SiC/Al that appear to have merit with respect to rotary engine applications include increased wear resistance [4] and lower thermal expansion behavior [2].

While improved mechanical and thermal properties of this discontinuous fiber-reinforced aluminum are the major motivator behind this applications evaluation study, other attributes of this class of MMCs represent potential improvements relative to practical engineering usage. The first of these is manufacturability. While discontinuous MMC's can achieve only a percentage of the unidirectional properties of continuous filament-reinforced composites, the random orientation of the SiC particles dispersed in the aluminum matrix results in a material which can have essentially isotropic properties. This characteristic should significantly aid in design, manufacturing and attachment considerations. A second

attribute is the variety of fabrication procedures employed to make these discontinuous SiC/Al materials. Casting, forging and extrusion processes are available for these materials. This allows for near-shape component fabrication, with associated reductions in final part machining requirements. Finally, this MMC has the potential of low cost, resulting from the use of relatively inexpensive constituents, aided by the above fabrication benefits, which also contribute to the low cost.

NASA has conducted an on-going program to study advanced rotary engine designs. In a study published in 1982, "advanced" and "highly advanced" stratified charge rotary combustion engine designs were evaluated [5]. The resultant engine-airframe integration study predicted substantial improvements in performance, weight, noise and cost factors, including a 30 to 35 percent lower fuel usage, for these advanced rotary engines. These improvements were predicated on the necessary technological advances, identified in the study, being achieved and implemented. The 1982 study identified a number of technological advances which would be of major importance in achieving the advanced rotary engine objectives. Among these were a higher, hot strength aluminum alloy for housing applications, a lightweight rotor, and improved apex seal/trochoid housing coating materials.

In state-of-the-art rotary engines, these components are fabricated from conventional materials. The trochoid housing is usually fabricated from A201, an aluminum casting alloy with good high temperature properties. The end housing can be fabricated from A242, another aluminum casting alloy. Stainless steel and modular iron are commonly employed as rotor materials. Aluminum has also been investigated for rotor applications but low stiffness, high wear and high thermal expansion constituted major limitations [21]. As Figure 2 illustrates, rotary engine housings also employ a high wear resistant coating to counter the actions of the rotor apex seal. Chromium and molybdenum are representative coating materials. Because of the thermal expansion mismatch that exists between these coatings and aluminum alloys, a stainless steel insert between the coating and the aluminum is employed. While this approach provides a solution to the sealing requirements of rotary engines, it obviously introduces weight and fabrication complexity penalties.

ORIGINAL PAGE
BLACK AND WHITE PHOTOGRAPH

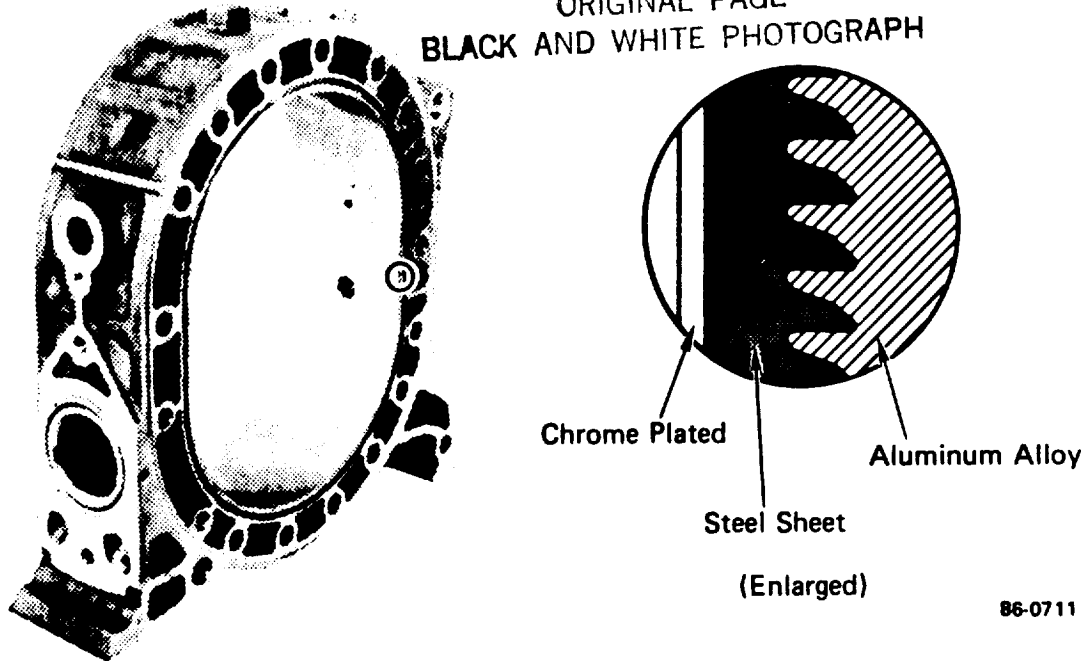


Figure 2. Cross-Sectional Representative of Rotary Engine Housing
(Reference 19)

The characteristics of SiC/Al, previously outlined, appear compatible with the technological advances needed for many components of "advanced" stratified charge rotary combustion engines. Strength improvements at higher temperatures for SiC/Al, if applied to housing components, could lead to higher engine operating temperatures and, hence, increases in performance efficiency. Additionally, a higher specific stiffness at temperature could lead to thinner, lighter weight housing designs; the lower thermal expansion behavior might mitigate the need for the stainless steel insert; and increased wear resistance might reduce the coating requirements. The property limitations that defeated the use of aluminum as a rotor material may be overcome by the higher stiffness, increased wear resistance, and lower thermal expansion behavior of SiC/Al. Substantial weight savings would result. Finally, the wear characteristics of SiC/Al could conceivably contribute to improved apex seal/trochoid housing coating designs and materials.

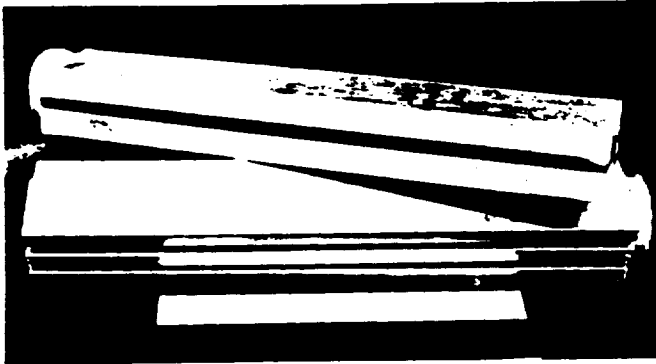
Based on this preliminary assessment, it would appear that SiC/Al has several characteristics that merit its investigation for application to rotary engine components.

Several vendors have been involved in the development of SiC/Al composites [6-10]. The majority of the fabrication processes employed have utilized powder metallurgy technology. A casting approach utilizing conventional aluminum foundry technology and silicon carbide grit appears to have attractive potential [9,10]*. The casting approach minimizes both the formation of interface oxides and retention of dissolved gases. It can produce an extremely uniform dispersion of particulates throughout the aluminum matrix (11). The means by which wetting is achieved between the SiC particles and the aluminum matrix is proprietary technology. The casting approach has major fabrication cost advantages, contributing to expectations that it should result in a low cost MMC. Additionally, as opposed to the powder metallurgy approach, the casting process offers additional cost advantages in the fabrication and machining of complex shapes. As Figure 3 illustrates, the fabrication techniques for this composite material are already in a fairly advanced state of development.

In summary, SiC/Al and especially the cast SiC/Al process, appears to have the potential of making major contributions to achieving the objectives of the advanced rotary engine program. This results from its promising material properties, the relative ease of fabricating complex shapes, and its cost potential. The critical need appears to be a materials testing program and preliminary design analysis study focused specifically on the rotary engine application. This preliminary evaluation study is the overall goal of this Phase I program. If the Phase I program is successful in identifying a rotary engine component which would produce significant overall performance benefits if fabricated from cast SiC/Al, the Phase II program would pursue engineering development of this component.

* Dr. David M. Schuster developed this process while at Scientific Applications International Corporation, La Jolla, California. Subsequently, the American subsidiary of Alcan, Ltd., acquired the rights to the process and has established the Dural Aluminum Composites Corporation (DACC) to further the development of this material.

ORIGINAL PAGE
BLACK AND WHITE PHOTOGRAPH

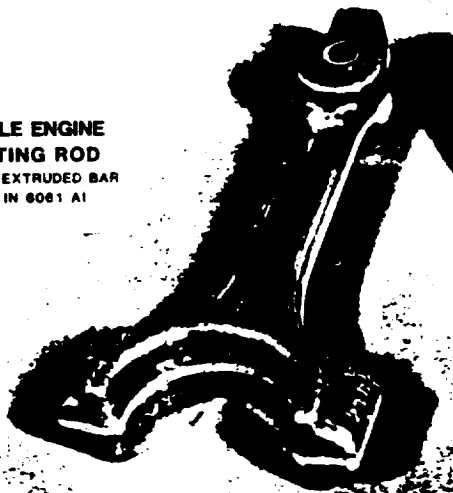


ROLLING

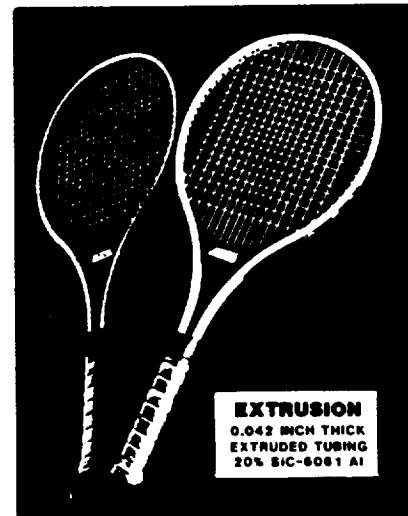


CASTING
TEN THREADED TENSILE BARS
CAST IN ONE MOLD
20% SiC-A357 Al

**AUTOMOBILE ENGINE
CONNECTING ROD**
FORGED FROM EXTRUDED BAR
15 v/o SiC IN 6061 Al



FORGING



EXTRUSION
0.042 INCH THICK
EXTRUDED TUBING
20% SiC-6061 Al

86-0712

Figure 3. Representative Casting Techniques for Cast SiC/Al

1.2 Phase I Statement of Work and Conducted Activities

As presented in the Phase I proposal[1], "the general objective of the Phase I program is to demonstrate that the cast SiC/Al material can make a significant contribution to the advanced rotary combustion engine program."

"The specific technical objectives are to: assess the feasibility and the benefits of making the trochoid housings from cast SiC/Al; determine what improved performance (housing) coatings are compatible with the cast SiC/Al; and evaluate other applications for the cast SiC/Al, such as end housings, the rotor and the apex seals."

The proposed Phase I work plan included the conduct of the following tasks:

1. Fabrication of SiC/Al Test Specimens

"Test specimens will be fabricated for high temperature tensile testing, fatigue testing and coefficient of thermal expansion (CTE) measurements. Two volume fractions of SiC loading will be considered."

10 volume percent (v/o) and 20 v/o SiC were selected as the volume fractions of the loading material. A201 aluminum alloy was selected as the matrix material. The composite was hot isostatically pressed (hipped) and heat treated to a T6 condition. The material test matrix was expanded to include DACC's hipped A201-T6 matrix material and commercially available A201-T6, both to provide reference properties data.

2. Mechanical Testing

The Phase I proposal specified limited mechanical testing consisting of tensile tests at temperature and some fatigue measurements. Duplicate tensile specimens at four temperatures for the two loading fractions was the proposed extent of the tensile testing program.

As a result of early materials quality problems, better definition of critical design problems and the desire to obtain a property data base more in accordance with the needs of the analysis effort, the mechanical test program was expanded significantly. The final evaluation and test program consisted of:

- a. metallography and radiography - conducted to provide quality assurance information on the SiC/Al billets;
- b. chemical analysis of billet inclusions;
- c. characterizing two forms of the matrix alloy - to better define the properties improvements provided by the SiC loadings;
- d. hardness tests - as a check on matrix quality;
- e. three tensile specimens tested at each test temperature (room temperature (RT), 300, 400 and 500°F; and
- f. a retest of some 20 v/o specimens, necessitated by poor billet quality.

Wear and long-cycle fatigue testing on the 20 v/o material were conducted under PDA's IRAD funds. 17-7 ph and 17-4 ph stainless steels, respectively, were used in these test activities to provide reference data. Fatigue data to 50 million cycles at RT was acquired for the steel and MMC along with fatigue data at 400 F for the MMC.

3. Thermal Property Tests

The proposal called for thermal testing to be limited to CTE measurements of the two SiC/Al materials.

The conducted thermal test program was expanded to also include:

- a. CTE measurements of the reference aluminum alloy.
- b. thermal conductivity measurements on the two SiC/Al materials.

In addition, since data from the initial CTE tests appeared questionable, these tests were repeated to assure high quality data.

4. Housing Coating Investigation

An analytical investigation of the compatibility between wear resistant coatings and the SiC/Al material was proposed.

Component evaluation emphasis was ultimately directed at the rotor, as opposed to the trochoid housing anticipated in the Phase I proposal. This reduced the criticality of assessing coating compatibility in the Phase I study. Additionally, the practice of employing stainless steel liners to achieve CTE matching with coatings in current engine designs further reduced the criticality of this problem in influencing an assessment of SiC/Al applicability for housing applications.

Activities in this task were ultimately restricted to reviewing NASA state-of-the-art studies in advanced coating materials[12] and assessing the CTE compatibility of these coatings with the SiC/Al material.

5. Evaluation of Possible Component Applications

The Phase I proposal called for an assessment of possible component applications as well as the conduct of a feasibility design study of one selected component.

After a review of engine components, the rotor was selected for detailed study. A generalized finite element model of a rotor was constructed using PATRAN[13] and thermal stress, static stress and fatigue

analyses were conducted for two loading conditions. A performance comparison of 17-4 ph stainless steel rotor versus a 20 v/o SiC/A201-T6 rotor was accomplished, utilizing an existing rotor design.

6. Reports

Monthly letters were proposed along with the contractually required final report.

All reporting requirements were fully met[14].

1.3 Summary

All tasks of the Phase I program were completed. All objectives of the Phase I program were attained.

The general conclusion of the Phase I study is that the cast SiC/Al MMC may generate significant performance benefits for rotary engines since viable applications appear feasible in rotor, end housing and trochoid housing components. This conclusion is reached, in part, based on the mechanical and thermal properties measured in the test program. These showed significant improvements in high temperature modulus, wear, high temperature fatigue and thermal expansion behavior relative to the properties of the A201-T6. The SiC/Al had no degradation in high temperature strength nor reduction in thermal conductivity relative to A201.

The specific conclusion of the Phase I study is that 20 v/o SiC/A201-T6 appears viable as a rotor material. The rotor feasibility design study disclosed no major limitations in the use of this material. If successfully developed, an SiC/Al rotor could achieve a total weight reduction in a rotary engine on the order of 17%.

Although the rotor design specifically studied in the Phase I program had been developed for stainless steel characteristics,* direct substitution of the stainless steel by 20 v/o SiC/A201-T6, in this design, based on thermal stress, static stress and fatigue analyses, indicated the following:

* It is anticipated that a rotor design, specifically based on SiC/Al characteristics, would demonstrate even stronger performance capabilities.

1. Mean static stress in the SiC/Al rotor was one-half of the mean static stress in a 17-4 ph stainless steel rotor;
2. The maximum static stress in the SiC/Al rotor occurred in the critical shallow pocket rib area in the Top Dead Center (TDC) position where the temperature is the highest.* Under the conditions of this design study and at this stress level, the factor of safety in static design was one. A rotor redesign would be expected to lower peak stresses or temperatures in this critical area, thus providing an acceptable safety margin.
3. Fatigue testing and response analyses suggest a life of 100 million cycles for a SiC/Al rotor compared to an infinite life for the steel rotor. Based on a continuous operation, at a crankshaft speed of 8000 RPM, this feasibility design study predicts a SiC/Al rotor life of about 600 hours. Again, a rotor redesign specifically based on SiC/Al properties should result in an operating life in excess of 3000 hours.
4. If a direct substitution of SiC/Al for steel is possible, the weight savings will be: 63 percent for the rotor; 51 percent for the counterweight; and 17 percent for the total engine.

Other accomplishments of the Phase I program can be categorized and summarized as follows:

Materials Development

1. Radiographic inspection of cast SiC/Al billets detected extraneous high atomic number particle inclusions. The vendor determined their source, changed fabrication procedures, and eliminated the problem.

* It is anticipated that a rotor design, specifically based on SiC/Al characteristics, would demonstrate even stronger performance capabilities.

2. Comparative testing of A201 alloys, commercially obtained versus as-processed-for metal matrix composite fabrication, indicated a nominal 10% reduction in strength and stiffness properties for the latter. This suggests material improvements in the MMC may be possible by improving alloy processing procedures.
3. Average properties may have been adversely affected by lack of uniformity in billet materials. Relatively large data scatter was observed in the test program. It is to be expected this problem will gradually be reduced as DACC gains additional experience in the processing of these materials.
4. For the rotary engine application(s) under investigation in this program, no "Achilles heels" were uncovered in fundamental characteristics of this material. This is an extremely important conclusion, signifying no major materials improvement are required to implement application of this material to the rotary engine.

Mechanical Properties

1. The strength and the modulus of the A201 alloy used in the MMC was degraded slightly from that available in commercial A201 alloys. This is attributed to processing procedures and not an inherent result of the SiC addition.

DACC notes that processing optimization studies to improve matrix properties have not been conducted[15].

2. No high temperature strength improvements were measured for the 10 v/o and 20 v/o SiC/A201-T6 relative to the properties of the base alloy. This is attributed to the low aspect ratio (3:1) of the SiC grit employed which inhibits effective low transfer from the matrix to the particles. In addition, no work hardening benefits were gained, as only a straight casting approach was used in billet fabrication.

The use of SiC particles with greater aspect ratios and/or the use of work hardening methods (grain boundary effects) in fabrication would be expected to result in high temperature strength improvements. Such improvements, however, are not considered to be a responsibility of the PDA program under discussion. All performance assessments in this study were made on the basis of no strength improvements at temperature for cast SiC/A201-T6.

3. Significant improvements in the elastic modulus of the SiC/Al material, relative to the base alloy, were produced and maintained to the maximum test temperature of 500°F. Considering the lower modulus of the matrix alloy relative to the commercial material (9.6 million psi vs 10.3 million psi), the values for the reinforced aluminum approximated rule of mixtures responses. At 500°F, moduli for the unloaded, 10 v/o and 20 v/o materials were 8.7 million psi, 10.7 million psi, and 12.7 million psi, respectively.
4. Wear resistance tests, considered critical to rotary engine applications assessment, were conducted under PDA IRAD funds because of Phase I resource limitations. The resultant data are considered proprietary to PDA. They will be provided to NASA under separate cover to assist in the evaluation of this proposed application.

In summary, the Taber wear test was employed. Only room temperature tests were conducted. 20 v/o SiC/A201-T6 was compared with 17-7 ph stainless steel, H1050 condition.

5. Fatigue resistance data was acquired on the 20 v/o SiC/A201-T6 at room temperature and 300°F under PDA IRAD funds. This data is also considered proprietary to PDA. The fatigue data will also be supplied to NASA under separate cover.

A rotating beam fatigue test was employed. Data was acquired to 50 million cycles. 17-4 ph H1025 stainless steel was also tested at room temperature for comparative purposes.

6. Hardness tests were conducted on the base alloy and the 10 v/o and 20 v/o MMC materials. Results were significantly lower than manufacturer's data on the commercial alloy. These results are believed associated with the non-optimum processing of the A201 base alloy in fabrication of the SiC/Al composites.

Thermal Properties

1. The thermal expansion of the SiC/A201-T6 is significantly lower, relative to the expansion characteristics of the base A201 alloy. This represents a very positive attribute for rotary engine components. For example, in the moderate temperature range of RT to 212 F, the CTE of the 20 v/o material is 50% lower than that of the base alloy. Over a temperature range of RT to 400 F, the CTE of the 20 v/o material is 33 percent lower than that of the base alloy.
2. No apparent decrease in the conductivity of the base A201 alloy resulted from the 10 v/o and 20 v/o additions of SiC grit. A decrease had been expected based on a rule of mixtures response. Lack of this decrease has very major, positive ramifications with respect to the use of this material in rotary engine applications. Both housing and rotor applications will benefit from the retained conductivity.

Component Evaluation

1. SiC/Al warrants consideration as a materials candidate for end housing and trochoid housing components. Although no preliminary analyses were conducted on these components, an assessment of the properties of the SiC/Al relative to the critical needs of these components suggests the following:

- (a) There is no penalty in thermal conductivity relative to A201, a major consideration in the thermal management problems of trochoid housing usage. Consequently, the higher modulus and lower CTE of the SiC/Al may translate into a more efficient housing component (e.g., thinner, reduced requirements for the component stainless steel insert, etc.). The asset of the higher wear resistance of the SiC/Al material for this application also merits investigation.
 - (b) The end housing's design constraints are not as rigid as those for the trochoid housing. Consequently, the advantages of the SiC/Al, as discussed for the trochoid housing, have additional utility for this application.
2. Other components, such as the apex seal, side seals, etc. were not addressed at all. Consequently, no specific conclusions can be drawn for the components. The wear resistance capability of the SiC/Al probably justifies an investigation for these seal applications.
 3. As discussed earlier, the specific conclusion of the Phase I study is that it appears feasible to utilize SiC/Al for rotors for rotary engines. Significant weight savings would result. Higher rotational speeds may also be possible, resulting in additional performance benefits.

Phase II Program

At the initiation of the Phase I study, three possible scenarios were anticipated as a result of the conduct of the Phase I study:

1. The SiC/Al MMC appeared promising for one or more component applications, but a serious material deficiency had been identified. The Phase II program would thus emphasize materials development activities to correct this deficiency.

2. The SiC/Al MMC appeared viable for a particular component, but the feasibility analyses had identified a critical design problem. The Phase II program would focus on detailed analysis activities supplemented by additional materials testing to correct this problem.
3. The SiC/Al MMC material and component application appeared extremely viable as a result of the Phase I assessments. The Phase II program would emphasize component fabrication and prototype testing.

Scenario 1 did not develop. The results of the Phase I study lie between Scenarios 2 and 3. Given that the Phase I study suggests the feasibility of an SiC/Al rotor, the appropriate Phase II program should consist of:

1. The development of a rotor design specifically utilizing the characteristics of SiC/Al, the objective being to obtain an adequate margin of safety based on thermal static loads and fatigue analyses. This development activity should be an iterative design and analysis study.
2. The conduct of additional mechanical testing to better define critical characteristics of the SiC/Al material. Additional information is needed on extended fatigue behavior and wear resistance at temperature. The elevated temperature creep properties of SiC/Al should be addressed.
3. Optimizing the SiC/Al material by addressing design performance of the rotor as a function of SiC loading fraction and by improving the processing of the base alloy.
4. Analyzing performance limiting engineering problems on the rotor such as the apex seal, slot wear and deformation,

rotor-bore alignment, and fatigue resistance. These analyses should be conducted in sufficient detail to constitute an engineering assessment of the rotor.

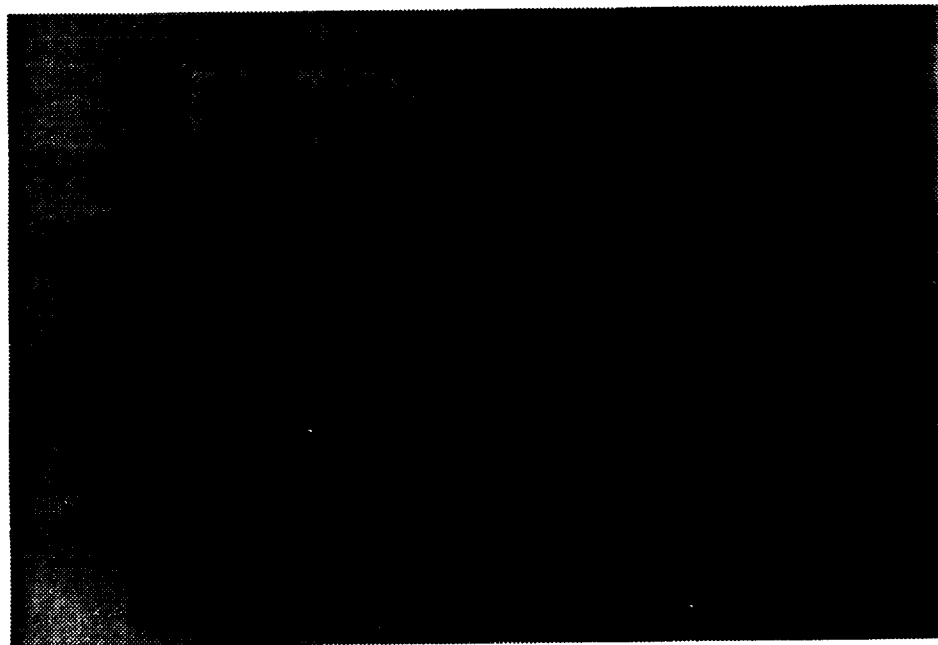
5. The development of a casting process for the SiC/Al material to accommodate the complex geometry of a rotor. Evaluation of this casting process should include both nondestructive and destructive testing. Sufficient iterations should be provided for this casting development program to result in a prototype rotor adequate for test purposes.

The ultimate deliverable product of the Phase II program, which will be proposed to NASA, will be a prototype SiC/Al rotor available for simulated and/or engine testing.

2.0 TEST MATERIALS AND PHYSICAL CHARACTERIZATION ACTIVITIES

2.1 Test Materials

The primary objective of the properties testing program was to characterize the cast SiC/Al materials. To this effect, two billets each, 3.5" x 10" x 1", of 10 v/o and 20 v/o SiC/A201 alloy, heat treated to a T6 condition, after being hot isostatically pressed (hipped), were acquired from Scientific Applications International Corporation (SAIC)(Figure 4).



86-0670

Figure 4. Billets of As-Received SiC/Al

To provide reference properties of the matrix material, a billet of A201-T6, subjected to hot isostatic pressing and to a T6 heat-treat condition was also acquired from SAIC. An ingot of A201, in a non-heat-treated condition, was obtained from the Consolidated Aluminum Company (CONALCO).

Radiographic inspection determined that all SiC/Al billets contained high density inclusions. The 20 v/o billets contained the greatest number of

inclusions, to the point where insufficient material existed for the full extent of the materials test program. Replacement billets were obtained from SAIC. Upon radiographic inspection, it was also detected that the A201-T6 billet acquired from SAIC had not been "hipped". A replacement A201 billet, subjected to the same hot isostatically pressing and heat treatment conditions as the SiC/A201-T6 materials, was subsequently obtained from the vendor.

In the wear and fatigue tests conducted by PDA under IRAD funds, 17-7 ph stainless steel (for wear tests) and 17-4 ph stainless steel (for fatigue tests) were also tested to provide reference data by which the SiC/Al material could be evaluated.

In summary, the materials for the test program were:

1. 10 v/o and 20 v/o SiC/A201, hiped, with T-6 heat treatment
2. A201, hiped with T-6 heat treatment, supplied by SAIC
3. A201 - CONALCO; T-6 heat treatment provided by PDA
4. 17-4 ph and 17-7 ph stainless steels

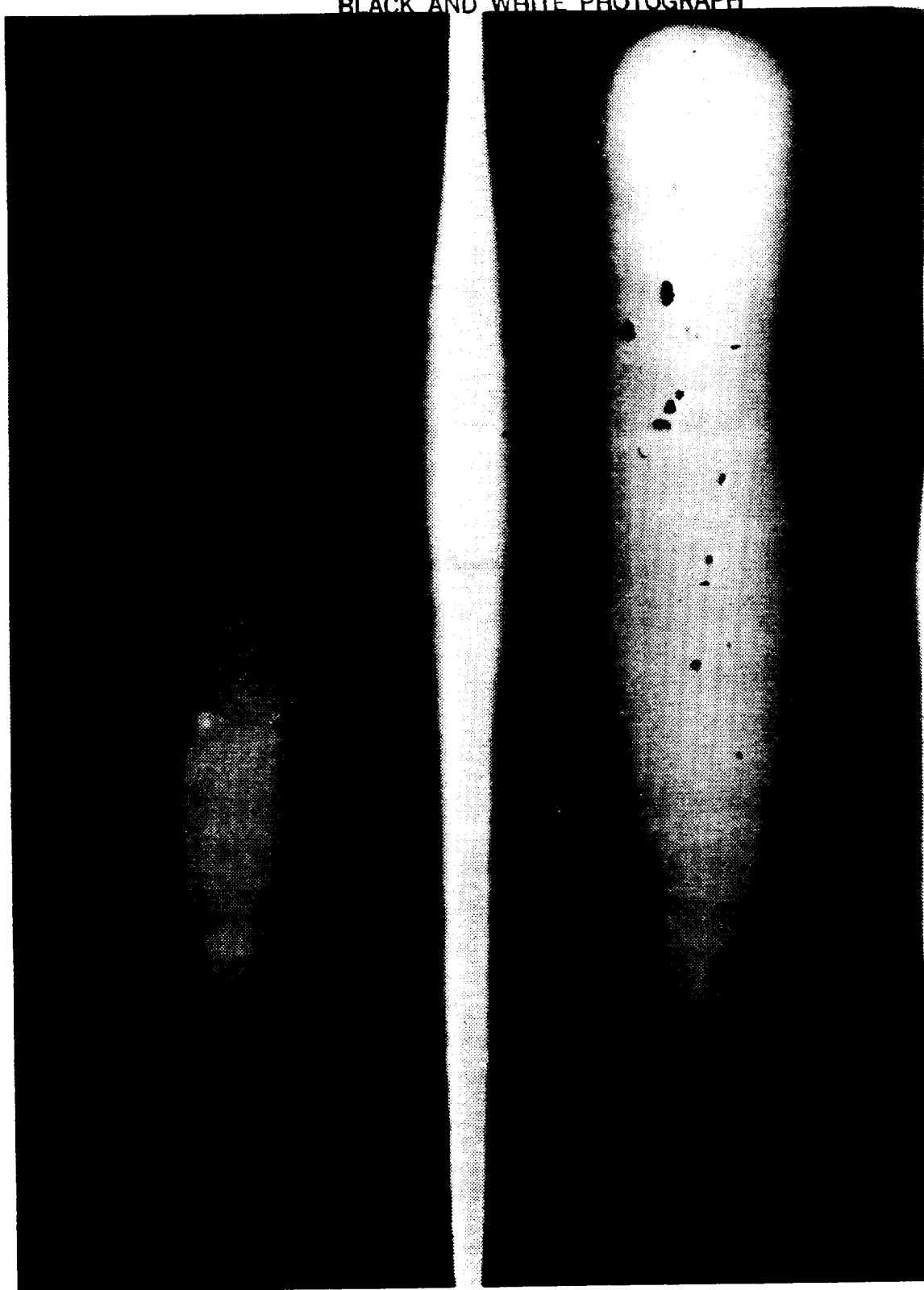
2.2 Physical Characterization

Radiography of the 10 v/o (Figure 5) and 20 v/o (Figure 6) billets was conducted to assess overall material uniformity. Radiography was also performed on the A201 billets obtained from SAIC.

In the x-rays of the SiC/Al composites, no obvious porosity defects were detected. There are smooth density variations and "grain" effects in the x-ray images resulting from thickness variations in the billets. The x-rays also showed many high density inclusions in the billets ranging from approximately 1/16" to 3/8" in thickness.

The detection of these inclusions created the first perturbation to the Phase I work plan. Optical microscopy, electron microscopy and x-ray analyses were performed to identify the inclusions. Micrographs of two high

ORIGINAL PAGE
BLACK AND WHITE PHOTOGRAPH

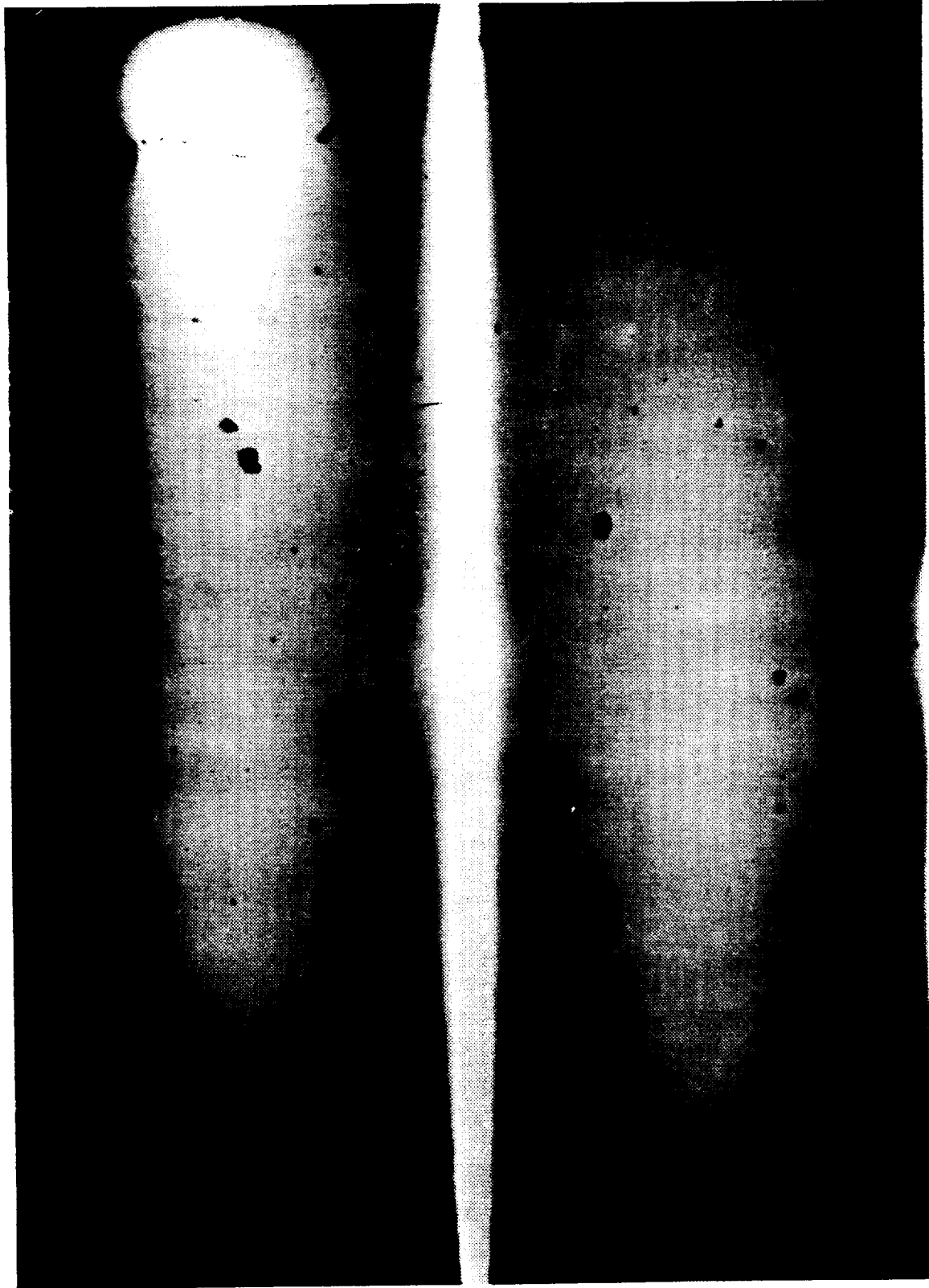


Billet #2

Billet #1

86-0674

Figure 5. Photographs of 10 v/o Billets



Billet #1

Billet #2

86-0673

Figure 6. Radiographs of 20 v/o Billets

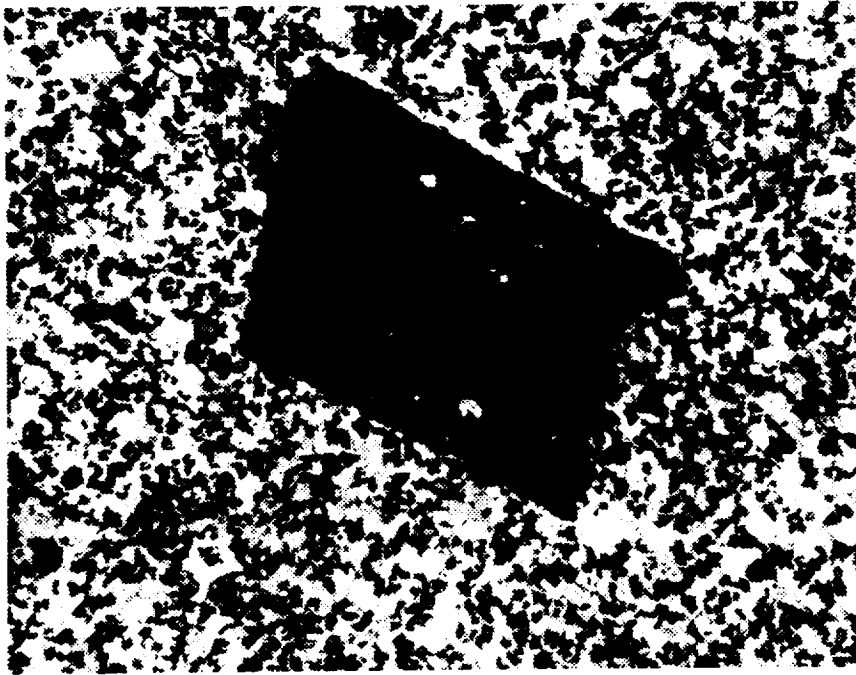
density inclusions contained in the 20 v/o material are presented in Figure 7. Both micrographs show a similar microstructure; a glassy interior material, surrounded by a reaction zone, grading into the unperturbed SiC/Al material. The inclusions were assessed as being inorganic compounds, one containing large amounts of zirconia.*

Given the population density of the inclusions in the 20 v/o billets, insufficient unflawed material existed to conduct the desired mechanical and thermal test program. DACC agreed to provide replacement 20 v/o billets.

Optical microscopy was also performed on the 10 v/o and 20 v/o billets to assess the general microstructure of the SiC/Al material. Representative photomicrographs, taken at 100 magnification, of the two materials are presented in Figure 8.

These micrographs indicate a tendency for the SiC particles to agglomerate at the grain boundaries of the aluminum. This provides a mechanism whereby work hardening would lead to a strengthening of the material. This grain boundary agglomeration tendency appears more pronounced for the lightly loaded, 10 v/o material. With the 20 v/o material, it is more difficult to assess the relative magnitude, if any, of the agglomeration effect of particles at the grain boundary. On a macroscopic basis, the dispersion of the particles throughout the matrix material appears to be reasonably uniform.

* In a meeting with D.M. Schuster, the casting process for SiC/Al was described as involving low pressures. Certain components of the casting mold employ a ceramic cement, in which an organic binder is used. It appears the molten SiC/Al destroyed the organic binder, sweeping ceramic particles into the melt. Recognition of this problem led DACC to replace the ceramic/organic cement with a non-reactive material. Radiographic inspection of the 20 v/o replacement billet would indicate this has solved the problem.



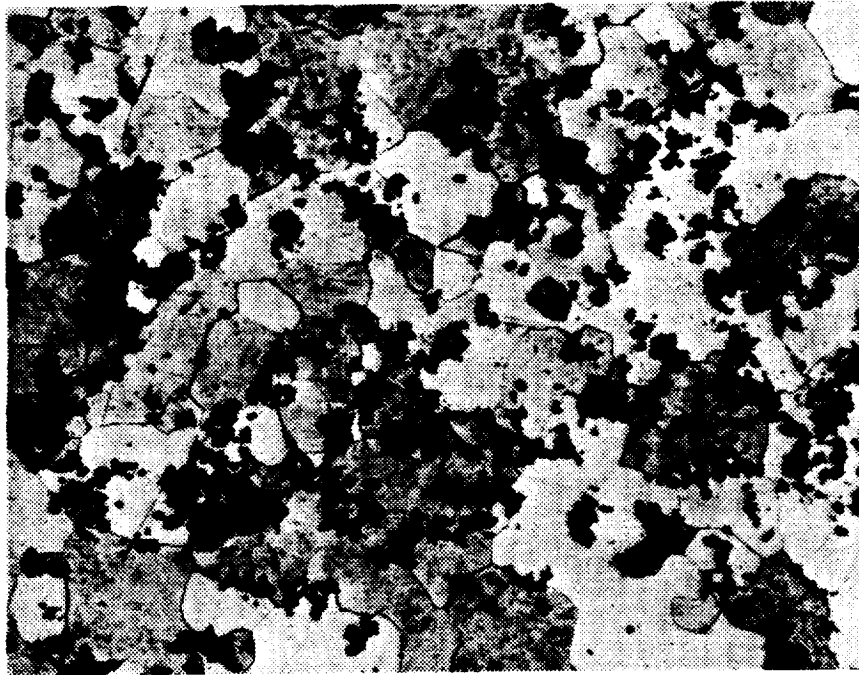
(b) 20% w inclusion



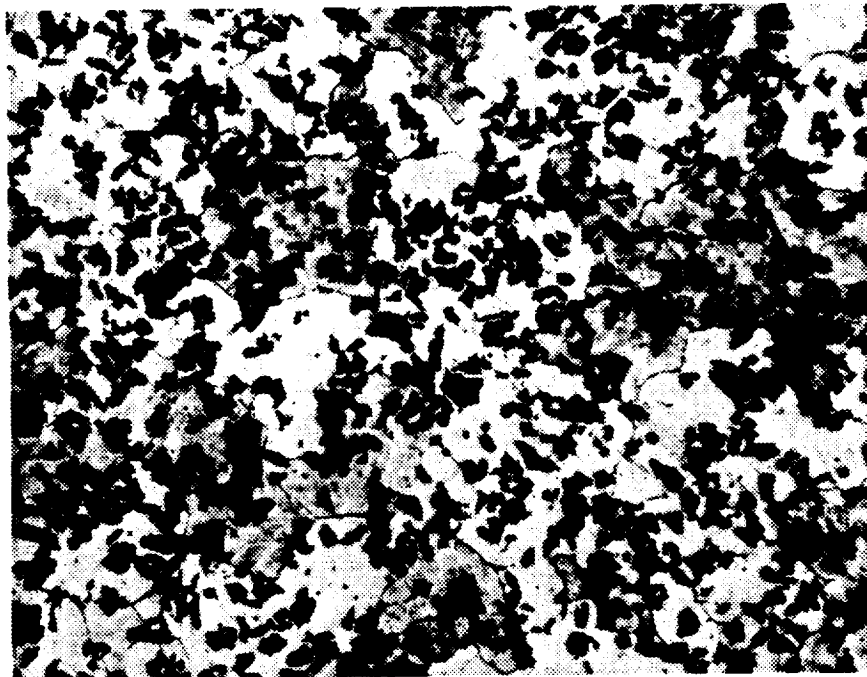
(a) 20% w inclusion

86-0671

Figure 7. Micrographs of High Density Inclusions in 20 v/o Billets



10 v/o



20 v/o

86-0672

Figure 8. Micrographs of 10 v/o and 20 v/o Billets, 100x

DACC utilizes a low-cost SiC grit as their loading material. Figure 8 indicates that the particle size employed has increased from the 10 v/o to 20 v/o material. This is believed to be a consequence of processing difficulties associated with higher volume fraction materials. This also suggests increasing difficulty may exist in the producing SiC/Al with loading fractions greater than 20 v/o.

Strength reinforcement of matrix materials requires a high aspect ratio for the reinforcing constituent to allow effective load transfer from the matrix to the reinforcing element to be attained. In metal composites, an aspect ratio of 10:1 is typically considered the lower limit for reinforcement constituent dimensions, below which this effective load transfer is not obtained. Examination of the micrographs (Figure 8) indicates typical aspect ratios for the SiC grit used in the DACC SiC/Al materials to be on the order of 3:1 or less. These aspect ratios are insufficient to achieve strength reinforcement. In addition, the casting process employed does not appear to have induced any orientation or alignment effects in the particle distribution which would have simulated the effect of higher aspect ratios. Therefore, it is anticipated that an effective strengthening mechanism will not be observed in these composite materials. *

* This constituted a major disappointment in our evaluation program. Specification literature issued by SAIC and, subsequently, by DACC indicates higher strengths are produced for their SiC/Al materials relative to the reference alloys. The conditions by which these strength increases were obtained by DACC are not known by PDA.

3.0 MECHANICAL PROPERTIES OF SiC/Al

3.1 Introduction

As a result of this Phase I program and PDA's IRAD funds, data was obtained on the hardness, high temperature strength and modulus properties, wear resistance at room temperature (RT) and fatigue resistance (RT and 400°F) of the cast SiC/Al material.

Overall, the mechanical testing program conducted exceeded that contained in the Phase I proposal. Some problems were encountered that adversely affected the resources allocated to this aspect of the Phase I program. PDA had no experience in machining of SiC/Al. The increased wear resistance of this material significantly increased the difficulty of machining specimens for the test program, necessitating a learning experience. PDA does not have an in-house high temperature, mechanical testing capability. The contract with the first service laboratory engaged to perform mechanical testing was terminated over procedural concerns based upon checkout tests. This necessitated the use of a second service laboratory with additional startup costs and wasted test specimens. Additionally, it was originally proposed to conduct mechanical tests to temperatures as high as 550 to 600°F. Equipment limitations and material response behavior revised the maximum test temperature to 500°F.

The test program that was achieved, however, more than provided an adequate base of material property data by which the feasibility design studies were conducted. It is important to recognize the relative soundness of the engineering materials property data used in these design studies. All material property data employed in the design analyses were directly obtained from this Phase I test program.

3.2 Hardness

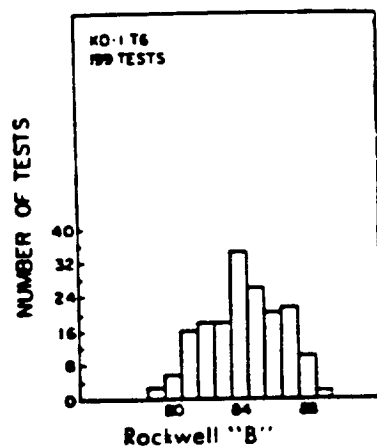
Hardness tests were performed on each of the materials tested to assess the heat treatment. Hardness values were measured on the Rockwell "B" scale at three points on each sample of material. Material samples were

selected at random, and no difference was found measuring hardness on a ground surface or a smooth as-cast surface. The averages of these values are tabulated in Table 1. Manufacturer's data for A201-T6 are presented in Figure 9.

Table 1
Hardness Values of A201-T6 Materials

Material	Hardness
A201-T6 (unhipped)	RB70
A201-T6 (hipped)	RB79
10v/o SiC/Al (hipped)	RB76
20v/o SiC/Al (hipped)	
Billets 1 & 2	RB85
Billets 3 & 4	RB75

Hardness values for all materials, except the first two billets of 20v/o SiC/Al, are low.* The technician conducting the tests stated that the accuracy of these tests on cast aluminum is within 15%. While this amount of uncertainty would allow actual hardness values to lie in the range of the manufacturer's data, it does not explain the consistently low values.



Reference:

Conalco Technical Information Report, CDRL-75-TIR-3, Composition, Properties and Metallography of Casting Alloy 201.

Figure 9. Manufacturer's Hardness Data for A201-T6

* Tensile tests on the higher hardness 20 v/o material did not show a significant increase in strength.

These low hardness values appear to be consistent with the slightly lower strength and stiffness properties measured on the base A201 alloy (see 3.3) relative to "handbook" properties. It is assumed all of these properties are a reflection of the non-optimized processing of the A201 alloy in conjunction with the fabrication of the MMC.

3.3 High Temperature Strength and Stiffness Properties

The tensile testing program was conducted at Truesdail Laboratories, Tustin, CA. The equipment used included an Instron model 1125 tensile test machine with a two pen recorder, a SATEK 3" I.D. furnace with temperature controller, a Measurement Group model 2100 signal conditioning system and one Micro-Measurements WK-06-125AD-350 strain gage bonded to each specimen. Room temperature (RT) data was taken at 74°F, while elevated temperature data was taken shortly after reaching the designated test temperature. Specimens were brought up to temperature in approximately one half hour. Specimen temperature was monitored continuously with two thermocouples, one at each end of the gage section. The temperature gradient across the specimen never exceeded 9°F and was usually 3-4°F. Three specimens were tested at each temperature. Test temperatures were RT, 300, 400 and 500°F.

The 0.2% yield strength data as a function of temperature are presented in Figure 10. The ultimate strength data as a function of temperature are presented in Figure 11. Manufacturer's and handbook property data on the A201-T6 alloy are presented in Appendix A.

The test results show some scatter, as well as a decrease in yield strength above 300°F when compared to reference data for A201-T6. Ultimate strength was almost always greater for the SiC/Al than for the A201-T6 alone. However, the ultimate strength of the A201-T6 material furnished by DACC was considerably lower than the reference data for A201-T6 material.

These data, along with the hardness data, would indicate the quality of the A201 material employed as the matrix constituent is not of an equivalent quality to the as-cast, commercially available A201 alloy. This

SILICON CARBIDE / .2% YIELD STRENGTH VS TEMPERATURE

○ A201-T6 (HIPPED) □ 10V% SiC/AL
◇ 20V% SiC/AL

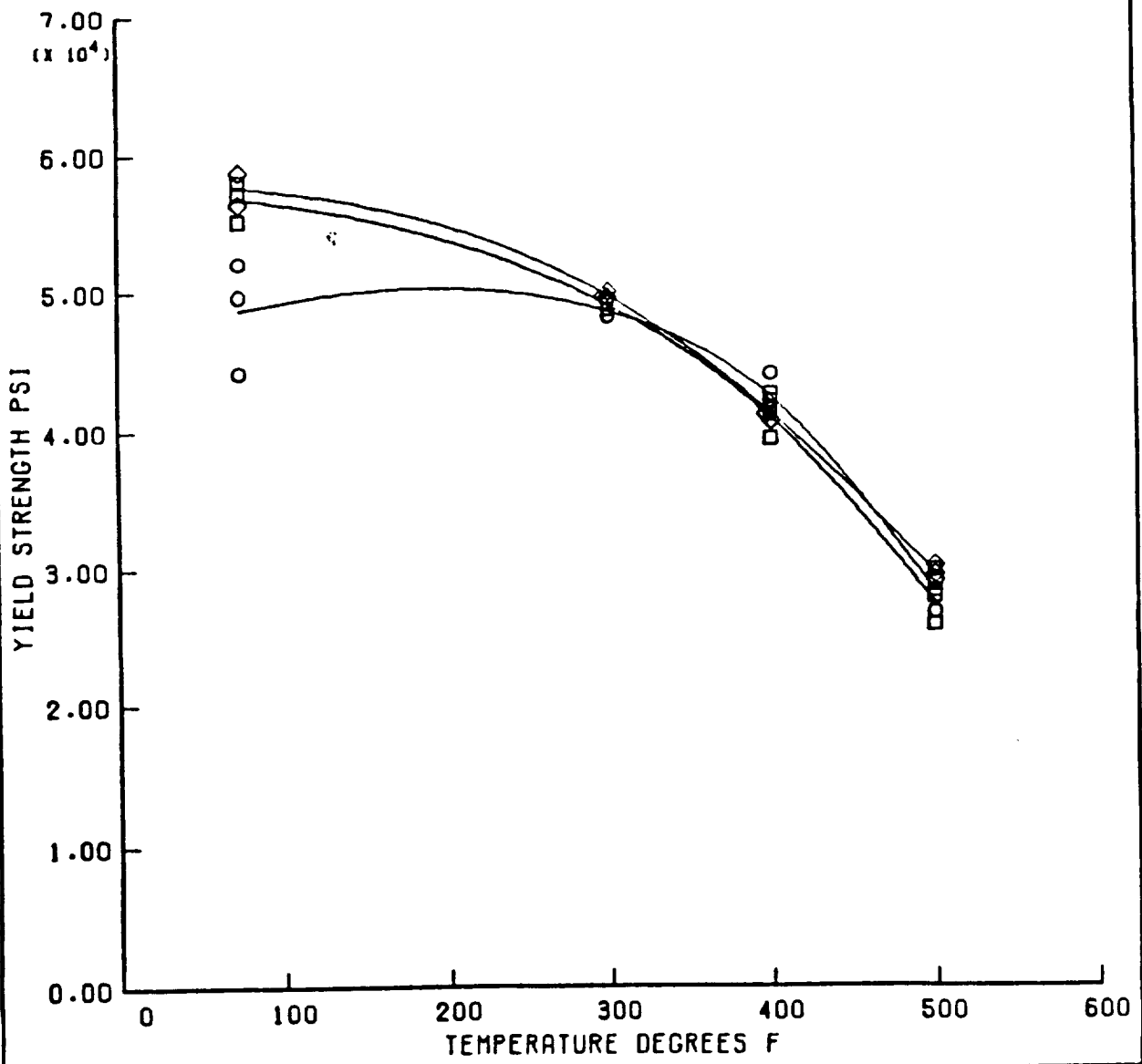


Figure 10. Yield Strength of SiC/201 Alloy

SILICON CARBIDE / ALUMINUM ULTIMATE STRENGTH VS TEMPERATURE

○ A201-T6 (HIPPED) □ 10VZ SiC/AL
◇ 20VZ SiC/AL

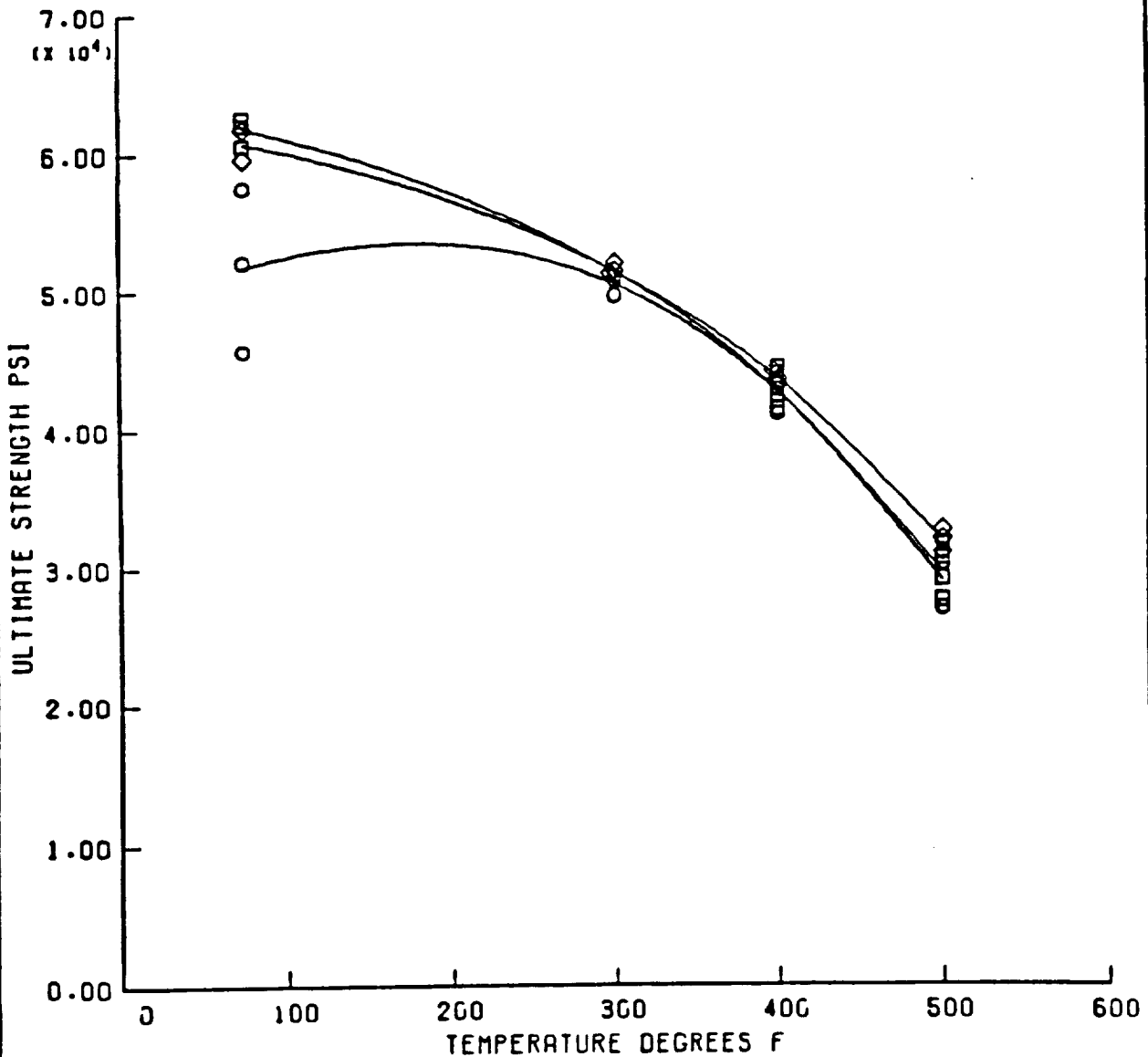


Figure 11. Ultimate Strength of SiC/201 Alloy

is, of course, not an unexpected result given the state of development for this material. It would suggest further improvements in material properties are achievable as better production processes are ultimately developed by DACC.

The average Young's modulus data for the three materials tested are presented in Figure 12. The discrete data points as well as the standard deviations are presented in Appendix B. The average value of 9.5 million psi for the unloaded A201-T6 is 8% lower than the reference value. (During check out procedures, the test apparatus indicated a room temperature modulus of 9.7 million psi for 6061-T6 aluminum. This is approximately 2% lower than the MIL-5-Handbook value of 9.9 million psi [16]).

Modulus values did consistently increase with increasing silicon carbide volume fraction. However, in elevated temperature tests, the shape of the stress-strain curve also changed as a function of silicon carbide volume fraction. The unloaded A201-T6 specimens show a long elastic region and a fairly well defined yield point. The 10 v/o suggests these specimens experience a plastic deformation at a lower stress and as a consequence have a more gradual yield behavior. These effects are slightly more pronounced in the 20 v/o specimens. This difference in stress-strain behavior is not noticeable at room temperature, but the trend is consistent throughout the high temperature data. This suggests that creep is taking place at the strain rate being used (0.02 in/in/min). These results also indicate that the creep properties of this material should be investigated.

3.4 Wear Resistance

Under PDA IRAD funds, wear tests were conducted to compare the wear characteristics of 20 v/o SiC/A201-T6 with a material similar to the 17-4 ph H1025 stainless steel used for the rotor in the NASA engine. These wear tests were also conducted at Truesdail Laboratories.

A Taber Abraser machine was used. This machine rotates a specimen approximately 3.5" square on a turntable at 70 rpm. Two free-turning

SILICON CARBIDE / ALUMINUM AVERAGE YOUNG'S MODULUS VS. TEMPERATURE

○ A201-T6 □ 10V% SIC/AL
◇ 20V% SIC/AL

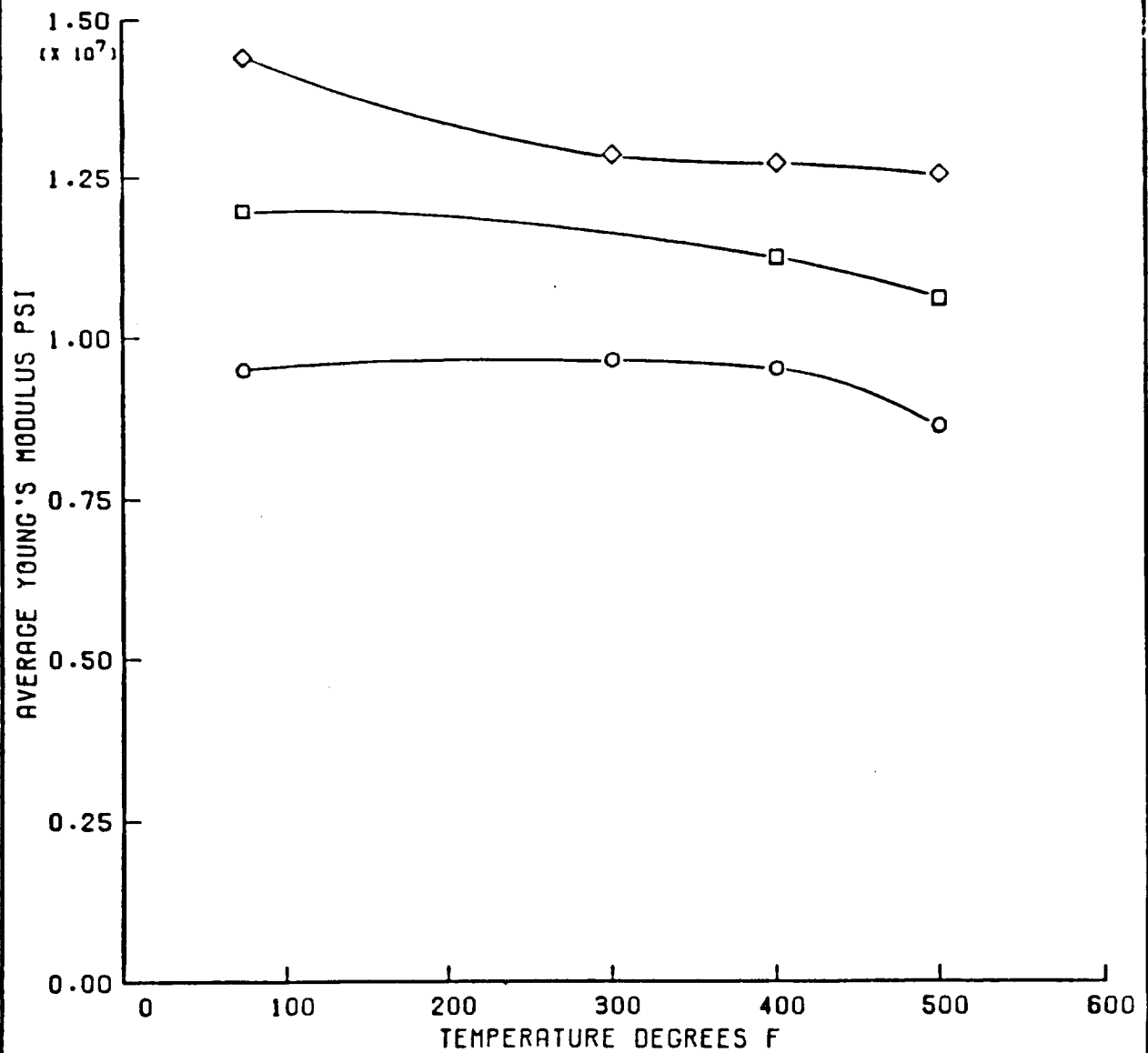


Figure 12. Average Young's Modulus for SiC/Al

abrasive wheels rest on the face of the specimen under pressure from dead weights. Specimens are weighed before and after testing to determine the material lost.

17-7 ph stainless steel was substituted for 17-4 stainless because of the ready availability of a small sample of the former material.

An IRAD report is in preparation documenting the results of these tests. A copy of this report will be provided to NASA-LeRC.

3.5 Fatigue Resistance

Under IRAD funds, PDA conducted fatigue testing of 17-4 ph stainless steel and 20 v/o SiC/A201-T6. The former material was tested at RT to about 50 million cycles. The latter material was tested at RT, to a maximum of 35 million cycles, and at 300°F, to a maximum of 15 million cycles.

Fatigue testing was accomplished using a rotating beam, high cycle fatigue test. The Rotating Beam Fatigue Testing Machine, Model RBF-2000, manufactured by Fatigue Dynamics of Dearborn, MI was used. Tests were conducted at Truesdail Laboratories.

Results will be published in a separate IRAD report. A copy of this report will be provided to NASA-LeRC.

4.0 THERMAL PROPERTIES OF SiC/Al

Because of the importance of thermal conductivity in trochoid housing applications, the Phase I program was expanded to include thermal conductivity measurements. These were made by the Thermophysical Properties Research Laboratory (TPRL), School of Mechanical Engineering, Purdue University.

As proposed in the Phase I proposal, thermal expansion tests were conducted on the 0 v/o, 10 v/o and 20 v/o SiC/A201-T6 materials. Similar to the problems experienced in mechanical testing, a second testing laboratory was ultimately employed to perform thermal expansion measurements.

4.1 Thermal Conductivity

TPRL performed thermal conductivity measurements on 10 v/o and 20 v/o SiC/A201-T6. Their complete report to PDA is included as Appendix C.

The bulk density (d), specific heat (C_p) and thermal diffusivity (α) were measured on each material. The thermal conductivity (λ) was calculated as a product of these quantities, i.e., $\lambda = \alpha C_p d$. These data are summarized in Table 2 along with available handbook information.

Table 2
Thermal Conductivity Measurements of SiC/Al

Sample Designation	Temp (°C)	Density (gm cm ⁻³)	Specific Heat (Ws gm ⁻¹ K ⁻¹)	Diffusivity (cm ² sec ⁻¹)	Conductivity (Wcm ⁻¹ K ⁻¹)
10 v/o	23	2.828	0.875	0.620	1.534
	75	2.828	0.910	0.582	1.498
	150	2.820	0.967	0.577	1.578
	225	2.828	1.000	0.597	1.688
	315	2.828	1.096	0.630	1.953
20 v/o	23	2.851	0.855	0.627	1.528
	75	2.851	0.902	0.588	1.512
	150	2.851	0.967	0.591	1.629
	225	2.851	1.000	0.588	1.676
	315	2.851	1.098	0.588	1.841
Hdbk A201	25	2.77	-----	-----	1.21
	100	-----	.921	-----	-----

The Metals Handbook [17] lists a conductivity for A201 (no heat treatment specified) of $1.21 \text{ W cm}^{-1} \text{ k}^{-1}$. The Engineering Data for Aluminum Structures handbook[18] indicates a range of conductivities for aluminum alloys of from 1.09 to $2.34 \text{ W cm}^{-1} \text{ k}^{-1}$.

A review of Appendix C and Table 2 indicates, somewhat surprisingly, that no penalty is incurred resulting in a decreasing the thermal conductivity of the base alloy by the additions of SiC. Also, there is essentially no difference in thermal conductivity between the two volume fraction materials tested. This deviation from the rule of mixtures response was a pleasant surprise.

In all conversations with John Deere Technologies, the criticality of maintaining the thermal conductivity of A201 for trochoid housing applications was emphasized. A sufficiently high thermal conductivity is needed to ensure proper heat management within the combustion chamber and at the housing surface. Feasibility design analyses showed this to also be an important material property for rotor applications. Thermal stresses are inversely proportional to the thermal conductivity. Consequently, these conductivity data are considered to be an important contributor to a favorable assessment of the usage of SiC/Al in rotary engine applications.

4.2 Thermal Expansion

Measurements of the thermal expansion of A201-T6, 10 v/o SiC/A201-T6 and 20 v/o SiC/A201-T6 were made by the Analytical Services Corporation of Irvine, CA and the Orange County Materials Test Labs of Santa Ana, CA. The former data are reported in Appendix D along with handbook data. A summary of the CTE results are presented in Table 3.

Table 3
Coefficient of Thermal Expansion Data
($10^{-6} \text{ in/in/}^{\circ}\text{F}$)

Temperature Range, $^{\circ}\text{F}$	Material System			
	A201-T6(Hdbk)	A201-T6(Dural)	10 V/O SiC	20 V/O SiC
122-212	10.8*	10.6	8.8	5.7
212-392	13.7	13.8	11.7	11.0
392-572	16.0	16.8	10.5	15.1
* 68-212 $^{\circ}\text{F}$				

It would appear that the data in the maximum temperature range for the 10 v/o material may be invalid. With that exception, the CTE data appears reasonable. These results also have several benefits with respect to rotary engine applications.

In the moderate temperature range of RT to 212°F, the 20 v/o material has essentially a 50% reduction in thermal expansion behavior compared to the baseline alloy. Over the probable temperature range of interests for rotary engine applications, RT to 400°F, the 20 v/o material has a 33% lower thermal expansion behavior compared to the baseline alloy.

The result should be a significant reduction in generated thermal stresses as a result of exposure to high temperature environments. This will also reduce the expansion mismatch between the wear resistant coating and the housing wall. It should also ease the rotor-bore misalignment problem due to thermal expansion differences.

5.0 COATINGS COMPATIBILITY

In the Phase I proposal, the assumption was made that the trochoid housing would be the primary component for applications assessment studies. Hence, an important issue was believed to be the mechanical, physical and thermal compatibility of the SiC/Al with wear resistant coatings applied to the trochoid housing. The Phase I proposal listed a specific task to address this subject.

The use of the stainless steel inserts between the housing material and the coating (see Figure 2) is a conventional practice, employed to minimize thermal expansion differences-induced problems. The use of this insert reduces the importance of the coating compatibility problem, regardless of the thermal expansion characteristics of the SiC/Al. Additionally, the applications assessment studies ultimately focused on the rotor, not the trochoid housing, further lessening the importance of this problem in a Phase I study. Consequently, while the Phase I proposal anticipated a design analysis of this problem, this effort was not justified in the conducted program.

The potential versatility of the SiC/Al materials for rotary engine applications indicates this problem ultimately will require design study. Consequently, compatibility with conventional housing coatings, such as chrome plating, nickel plating containing silicon carbide, or combined carbide or molybdenum alloys [19] is of interest. In addition, NASA has sponsored another SBIR study which addressed the potential of an adiabatic rotary engine [12]. This study identified Cr_2O_3 and ZrO_2 as ceramic coatings of potential interest to this type of engine.

The key issue in coating compatibility should be the magnitude of the mismatch in thermal expansion behavior that exists between the materials of interest. Presented in Table 4 is a comparison of the CTE values for the materials of interest for rotary engine applications. Clearly, the 20 v/o SiC/A201-T6 constitutes a significant reduction in the mismatch in thermal expansion behavior. Given the improvement in CTE in-going from 10 v/o SiC/A201 to 20 v/o SiC (i.e., 8.8 to 5.7), even higher volume fraction materials, if they can be fabricated, would be of interest to this problem.

Table 4

A Comparison of CTEs* for Materials
of Interest - Rotary Engine

<u>Al</u>	<u>Iron</u>	<u>Chrome</u>	<u>Molyb.</u>	<u>SiC</u>	<u>Cr 0</u>	<u>Zr0</u>	<u>20v/o SiC/A201</u>
13	5.5	3.9	2.8	4.5	4.5	5.8	5.7

* 10^{-6} in/in/°F at R.T

6.0 EVALUATION OF POSSIBLE COMPONENT APPLICATIONS

As noted in the introductory section, at the time of the Phase I proposal preparation, it was assumed that, because of the high temperature properties of SiC/Al, the trochoid housing would be the logical rotary engine component to receive a preliminary design study. The proposal did provide the option of selecting another component for evaluation based on the information acquired in the early stages of the Phase program.

There are at least four components in a rotary engine that are possible candidates to employ the SiC/Al material. These are the trochoid housing, the end housing, the (rotor) apex seal, and the rotor.

6.1 Trochoid Housing

The A201 alloy currently used for the trochoid housing, obviously, has acceptable properties. Its major disadvantage is a low wear resistance, necessitating the use of coating materials for interior surfaces of the housing. This, in turn, requires the use of a stainless steel liner to separate the two components, because of the thermal expansion mismatch between aluminum and the coating materials.

The anticipated merits of the SiC/A201 for this application were expected to be primarily in increased strength properties at temperature[1]. This was hypothesized to allow the rotary engine to run at higher temperatures and, hence, achieve higher operating efficiencies[1]. Lack of the strength increase at temperature has already been noted. Although, PDA has not conducted a thermostructural analysis of the A201 alloy for the trochoid housing application, it is reported by John Deere personnel not to be strength limited at current operating temperatures. Furthermore, higher engine operating temperatures, desirable from a performance efficiency standpoint, might present significant apex seal and coating wear problems[20].

Early component evaluation activities in the Phase I program focused on the trochoid housing. The complexity of the housing structure from an

analysis standpoint, the complexity of the housing structure from a fabrication standpoint, and recommendations by John Deere personnel of higher payoffs from other applications led to the decision to reduce the priority of this component with respect to evaluation. This position was reinforced when high temperature mechanical tests indicated improvements in strength properties had not been obtained.

Regardless, as a long term activity, it is amply justified to consider SiC/Al as a materials candidate for the trochoid housing. Even with no improvement in tensile strength, the SiC/A201-T6 material is a potential candidate for the following reasons:

1. in the critical area of heat transfer (i.e., thermal conductivity), its use incurs no penalty;
2. with a significantly higher modulus than the baseline alloy, approaching 50% for the 20 v/o material, the same applied loads will result in significantly lower deflections. Reductions in wall thicknesses may be possible, resulting in weight reductions.
3. the lower CTE along with its increased stiffness reduces the expansion incompatibilities with the wear resistance coatings. It may be possible to eliminate the stainless steel liner.
4. more speculative possibilities include the wear resistance characteristics of the SiC/Al and the potential of developing a higher-strength-at-temperature material.

Whether these result in significant performance benefits relative to the added material costs would require a detailed engineering study.

It would appear that to obtain performance benefits in addition to the above hypothesized weight reductions, such as higher operating temperatures, the development of a cast SiC/A201-T6 material with increased

high temperature strength properties, will be required. While such a material property appears obtainable, it would probably require the usage of higher priced silicon carbide whiskers as opposed to the silicon carbide grit now employed in the DACC material.

6.2 End Housing

The end housing appears to be an attractive candidate for SiC/Al, if adequate cost benefits can be established.

John Deere reports that a rotary engine developed by the Israeli's has an aluminum end housing that does not utilize wear-resistant coatings. This would suggest that, on higher performance engines that now require coatings on the end housings, the SiC/Al material may provide an adequate wear resistant surface, thus eliminating the need for coatings.

As in the trochoid housing application, the higher stiffness of the SiC/Al could allow housing thicknesses to be reduced. Detailed design studies would be required to assess the relative merits of this design improvement.

6.3 Seals - Apex, Corner and Side

"The gas sealing mechanism for the rotary engine consists of a side seal corresponding to the compression ring of the reciprocating engine, an apex seal to seal each working chamber from its adjacent ones, and a corner seal used at the junction of the above two seals" [19]. A self-lubricating special carbon (steel) has often been used for the apex seal. The side seal is usually made of a special cast iron. The corner seal is generally of a special cast iron with its outer surface chrome-plated to improve wear resistance of the seal diameter and the rotor seal hole.

Given that wear resistance appears to be the dominating material characteristic for these seal components, it would appear logical that the

SiC/Al could be a replacement material candidate. Possible advantages to its use in these seal applications would be weight reduction and perhaps a reduction in fabrication complexity.

6.4 Rotor

Current rotary engine designs employ nodular iron or stainless steel as rotor materials. If SiC/Al is practical as a rotor material, approximately a 60% savings in rotor weight (2.8 gm/cc vs 7.1 gm/cc) would be obtained. Additionally, since rotor engine designs employ counterbalancing weights on the rotor shaft to balance the inertial forces, then the use of SiC/Al as a rotor material could lead to a significant overall weight reduction in the rotary engine itself.

In the mid-sixties, the predecessor to the John Deere Rotary Engine Division, the Curtiss-Wright Corporation experimented with an aluminum rotor [21]. It is important to note that the major design limitation of the aluminum rotor was not its high temperature strength properties. Wall thicknesses could be increased to accommodate the lower strength of the aluminum. This, of course, essentially negated the density advantages of aluminum. However, two other problems influenced by wear resistance, stiffness and CTE characteristics, served to preclude the use of aluminum.

One problem was maintenance of the alignment of the rotor. With an iron or steel rotor shaft being used, the thermal expansion mismatch at the rotor bore between the aluminum and ferrous materials made it difficult to maintain rotor alignment. Some innovative mechanical design approaches mitigated this problem[22]; nevertheless, it remained a major hindrance to the use of aluminum rotors.

The other problem involved the wear resistance and the bowing of the rotor at the apex seal location induced by the resistance forces of the apex seal on the rotor housing. The origins of this problem lie in the poor wear resistance of aluminum and its relatively low modulus, resulting in high deformations under the resultant bending loads.

These problems have not yet been subjected to a comprehensive quantitative analysis (see Section 7) or specialized testing to determine the extent to which SiC/Al could mitigate or eliminate them. However, the mechanical properties (i.e., increased wear resistance and fatigue resistance, higher stiffness) and thermal properties (i.e., lower CTE) of SiC/Al are all favorable attributes to achieving solutions to these problems. The feasibility design study of an SiC/Al rotor, discussed in Section 7, uncovered no other major problems in the usage of this material.

7.0 FEASIBILITY DESIGN STUDY - SiC/Al ROTOR

7.1 Overview

Based on the recommendation of John Deere Technologies, the rotor of the NASA-Lewis rotary engine was selected for analysis. The NASA rotor is constructed from 17-4 ph stainless steel and has a compression ratio of 7.5:1.

The analysis approach was to construct a finite element model of the rotor. John Deere Technologies proprietary design information of the rotor was protected. Static analyses under several types of loading were conducted to determine the cyclic stress history of the rotor. Loading information was provided by John Deere Technologies.

No attempt was made to modify the design of the NASA rotor to accommodate the characteristics of the SiC/Al.

7.2 Finite Element Model

The geometry used for the finite element model was based on the NASA drawing of the rotor[23]. The model, Figure 13, is of a 1/4 rotor and was constructed using quadrilateral shell elements. The model contains 1734 elements, 1561 nodes and 9366 degrees of freedom. The model was constructed with PATRAN[13].

The flank and scoop cavity were modeled as being symmetric. An apex seal slot was added to investigate the relative deformations between a steel rotor and an SiC/Al rotor in the apex seal area (See 6.4). Symmetric boundary conditions were applied to the model in order to analyze a complete rotor.

7.3 Analyses

Analyses of the finite element model were conducted in order to construct a cyclic stress history for the rotor, similar to the one illustrated in Figure 14. These stress profiles, together with fatigue

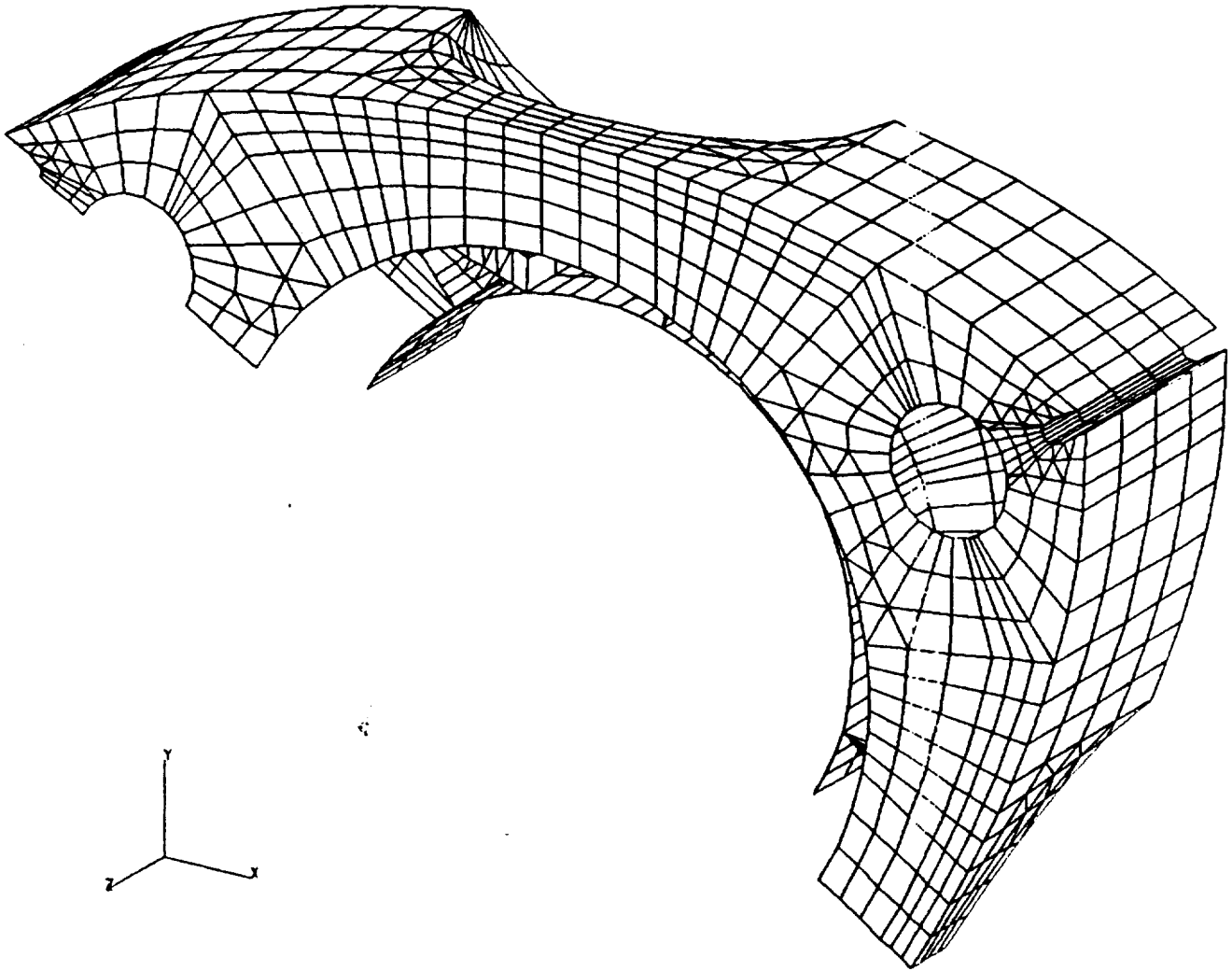


Figure 13. Finite Element Model of NASA Rotor

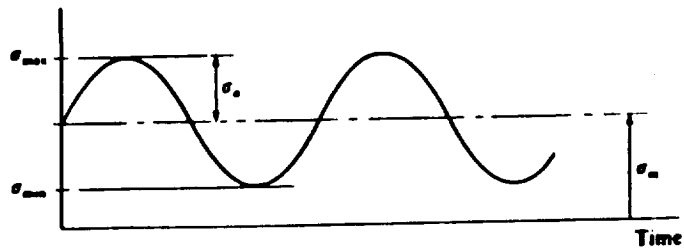


Figure 14. Cyclic Stress Profile

resistance data, will provide a comparison of cycles in failure for the baseline material (17-4 ph stainless steel) and the SiC/Al. In addition, the analyses will provide information on: the highly stressed regions; critical thermal expansion regions, such as the rotor-bearing bore; and critical deformation regions, such as the apex seal slot.

There are three basic loads present on the rotor; gas pressure, inertial, and thermal. These load conditions were analyzed at two specific crank angles to obtain cyclic stress information. The crank angles analyzed were Top Dead Center (TDC) and Bottom Dead Center (BDC). Each of the load conditions were analyzed separately at these crank angles. Then, by means of superpositioning of the stresses, the cyclic stress profile is obtained.

In the TDC load case, pressure loads are generated by the combustion and compression of the fuel. The centrifugal accelerations are generated by the rotation of the rotor about it's own axis. The translational acceleration is due to the eccentricity of the rotor's rotation about the crankshaft. The thermal loads are generated by thermal gradients set up by the expansion and cooling of hot combustion gases. The BDC load case contains all of the same loading components except the pressure.

The loading conditions were provided by John Deere Technologies. John Deere also provided film coefficients along with gas and oil reference temperatures in order to perform a convective thermal analysis and to generate a temperature distribution over the model.

Each load case was analyzed in two steps. The first was static analyses with pressure and/or acceleration/loadings. The second was a static analysis with thermal loads. Superposition was then used to obtain the predicted stress values. All analyses were conducted with the ANSYS finite element analysis program [24].

7.3.1 Thermal Analyses

The thermal analyses of the rotor was conducted in two steps. The first step was the determination of the equilibrium temperature distributions in the rotor for each material. Convective film coefficients, provided by John Deere Technologies, were applied to the rotor surface together with the corresponding reference temperatures and a heat balance was conducted using ANSYS[24]. The resulting temperature distributions are as shown in Figure 15. As this figure illustrates the steel rotor's hot spots reach peaks near 700°F while the peak temperature of the SiC/AL rotor's peak approaches only 450°F. The much lower peak temperatures in the SiC/AL rotor can be attributed to the higher conductivity of the SiC/AL material compared to steel. For example, at 400°F, the conductivities for 20 v/o SiC/A201-T6 and 17-4 ph steel are 8.07 and 0.899 Btu hr⁻¹in⁻¹F respectively.

The second step was the calculation of thermal stresses. Using the temperature distributions and values of CTE and stiffness for each material, the thermal stresses in the rotor were calculated using ANSYS. The peak stresses occurred in the pocket areas, and the shallow ribs supporting the pocket. In these critical areas the stresses for the SiC/AL rotor were about 1/2 the magnitude of those present in the steel rotor, as shown in Figure 16. Contributing to this difference was the lower peak temperatures and stiffness of SiC/Al material compared to steel.

7.3.2 Static Analyses

Static analyses were conducted on the rotor model in both the TDC and BDC positions. In the TDC position, the mechanical loads on the rotor were gas pressure, centrifugal and translational accelerations. These loads, which were also provided by John Deere Technologies, were applied to the model as shown in Figure 17. The bearing reaction forces were applied on the inner surface of the hub in order to satisfy conditions of static equilibrium. These reaction forces are depicted as a single vector in Figure 17; however, they were applied as a distributed force normal to the hub surface. The loads due the translational and centrifugal acceleration were

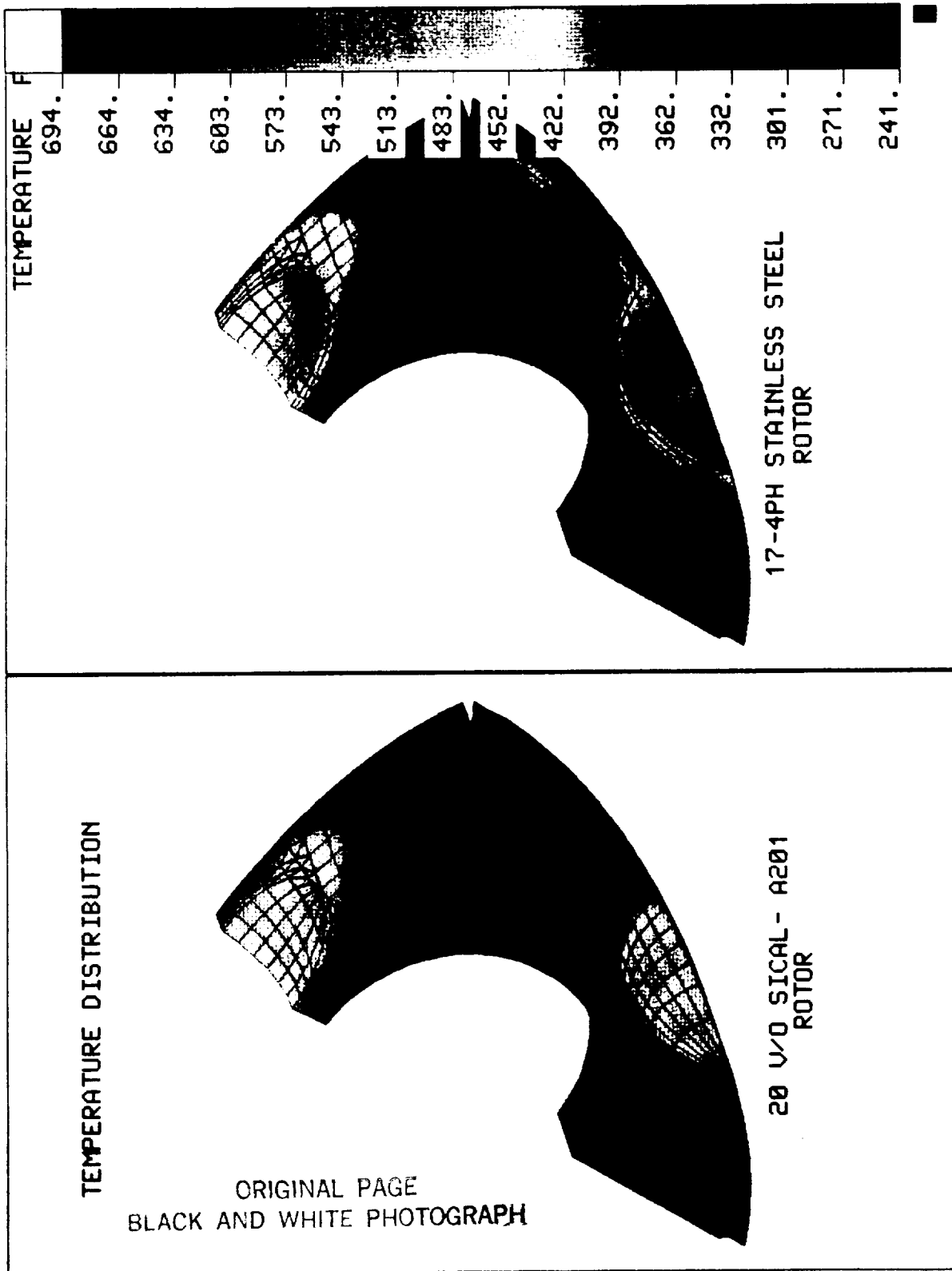


Figure 15. A Comparison of Temperature Distributions in SiC/Al and Stainless Steel Rotors

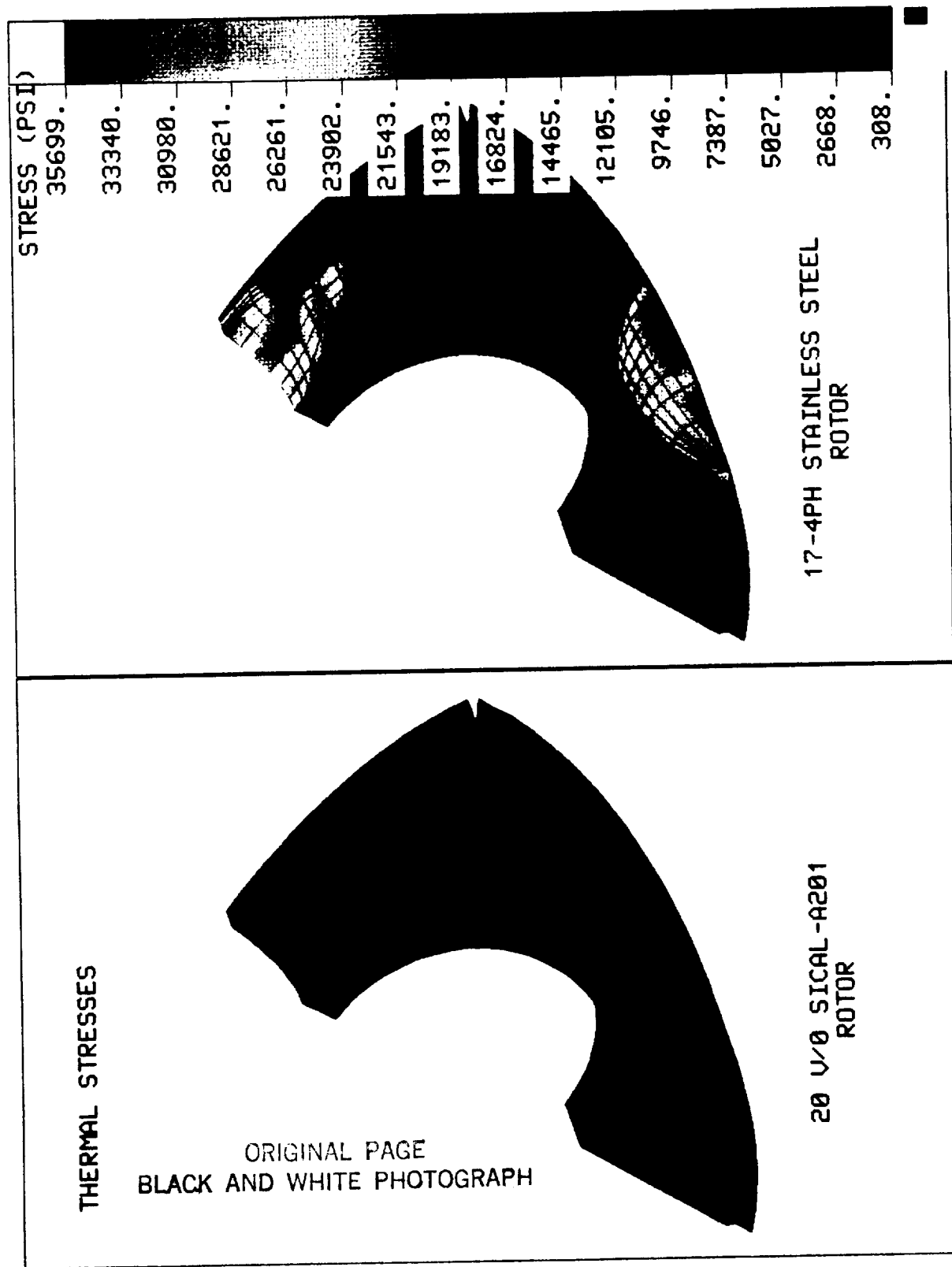


Figure 16. A Comparison of Thermal Stresses in SiC/Al and Stainless Steel Rotors

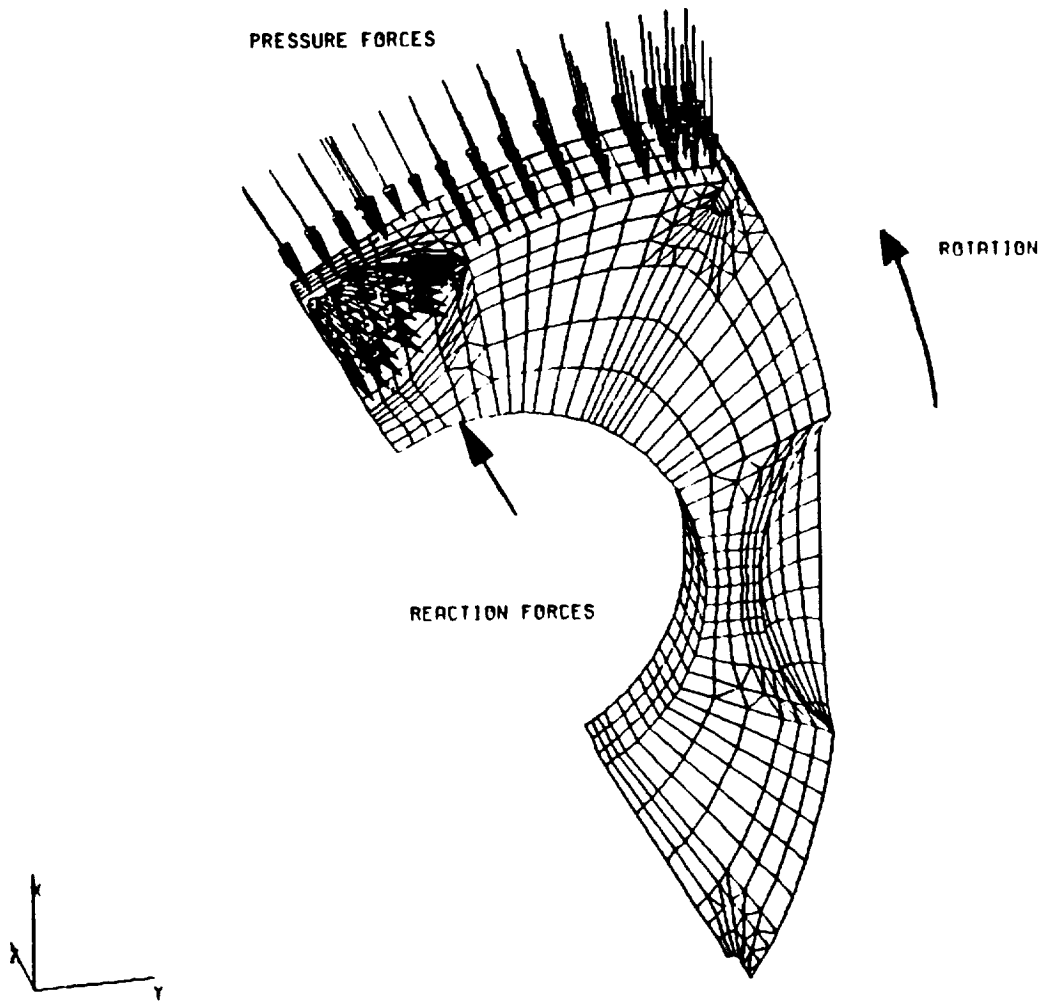


Figure 17. Top Dead Center Applied Loads

applied by constraining the rotor's translational motion and applying a translational acceleration and a angular velocity to the rotor. The translational acceleration was calculated from the rotors eccentricity and angular velocity.

The results of TDC static analyses, as shown in Figure 18, indicate that the pocket and shallow rib area are again the critical stress locations. The magnitude of the peak stress values for both the steel and SiC/Al rotors are approximately 19-20 Ksi.

In the BDC position, the only mechanical loads that were applied to the model are the translational and centrifugal accelerations. These loads were applied in the same manner as the TDC case. The results, shown in Figure 19, reveal that the stresses in the SiC/Al rotor are much lower than those in the steel rotor. These differences can be attributed to the substantially lower weight (density) of the SiC/Al rotor.

7.3.3 Fatigue Analyses

With the completion of the static and thermal analyses, the critical areas of the rotor were identified as the pocket and shallow pocket rib. Superimposing the results from the mechanical and thermal analyses, total equivalent stresses were calculated for both the SiC/Al and steel rotors in these critical areas. Cyclic stress profiles were then generated using the results from the TDC and BDC case together with the model's symmetry. One such profile, for a critical area in the shallow pocket rib is shown in Figure 20. This figure shows the stress levels that the rib will experience during one rotor revolution. Table 5 lists the mean stress (σ_m) and amplitude stress (σ_a) for both the steel and SiC/Al rotors in the shallow rib location of Figure 20.

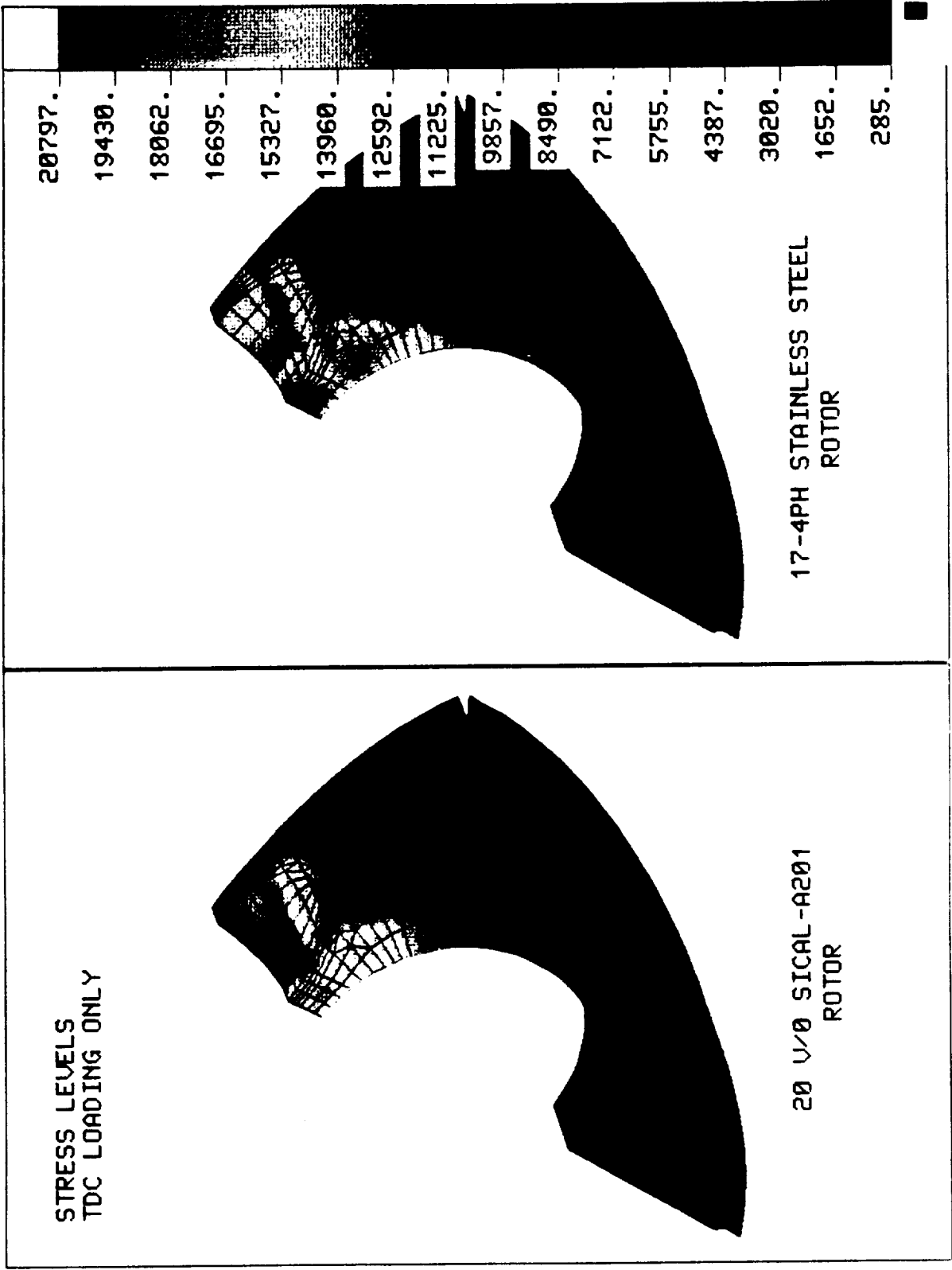


Figure 18. A Comparison of Static Stress Levels (TDC Condition) in SiC/Al and Stainless Steel Rotors

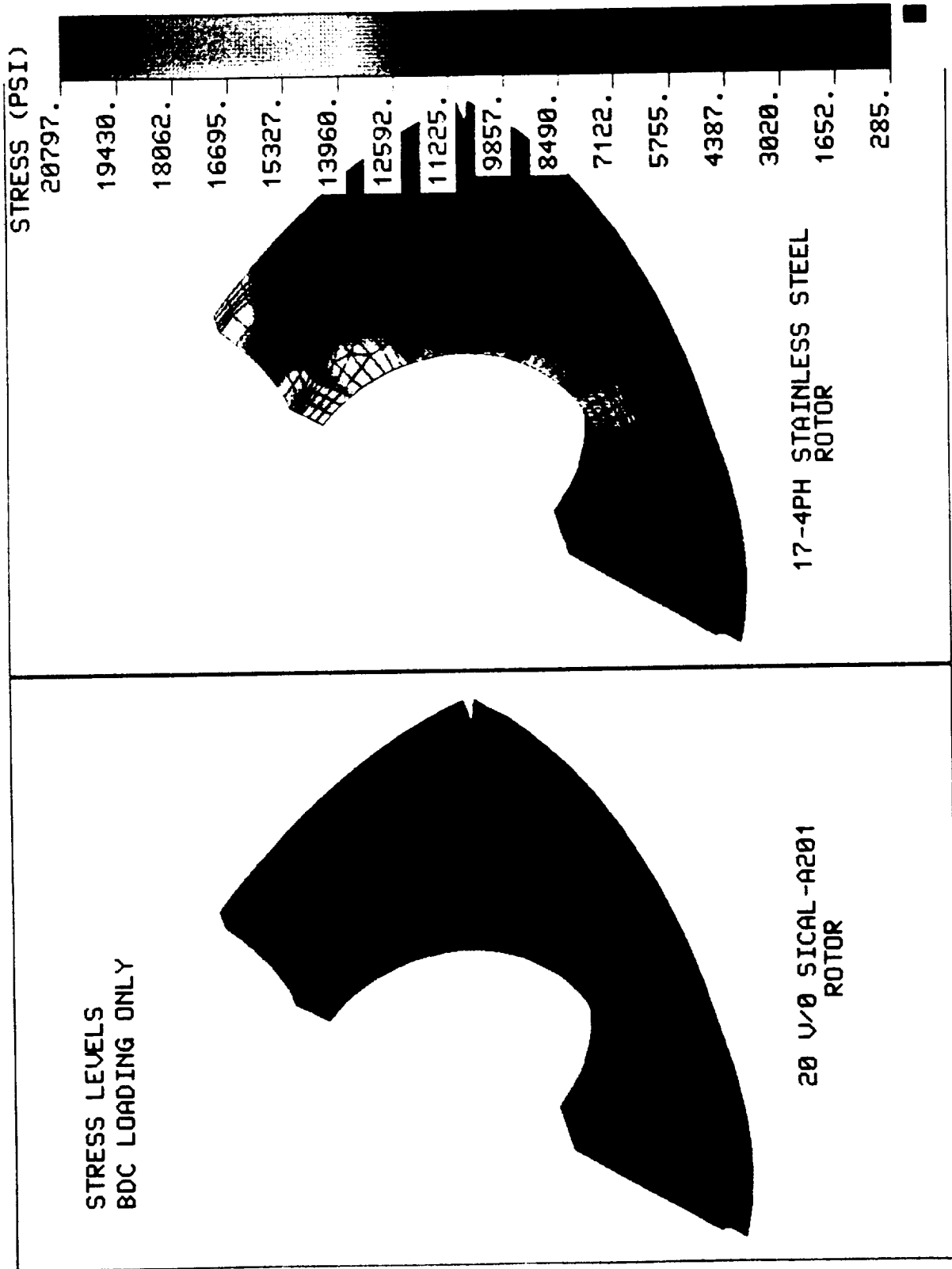


Figure 19. A Comparison of Static Stress Levels (BDC Condition) in SiC/Al and Stainless Steel Rotors

NASA 40 CU. IN. ROTARY ENGINE ROTOR
PRESSURE(TDC)=1400 PSI SPEED=8000 RPM

○ 17-4PH STAINLESS STEEL ROTOR

□ 20 V/8 SiC/AL-A201 ROTOR

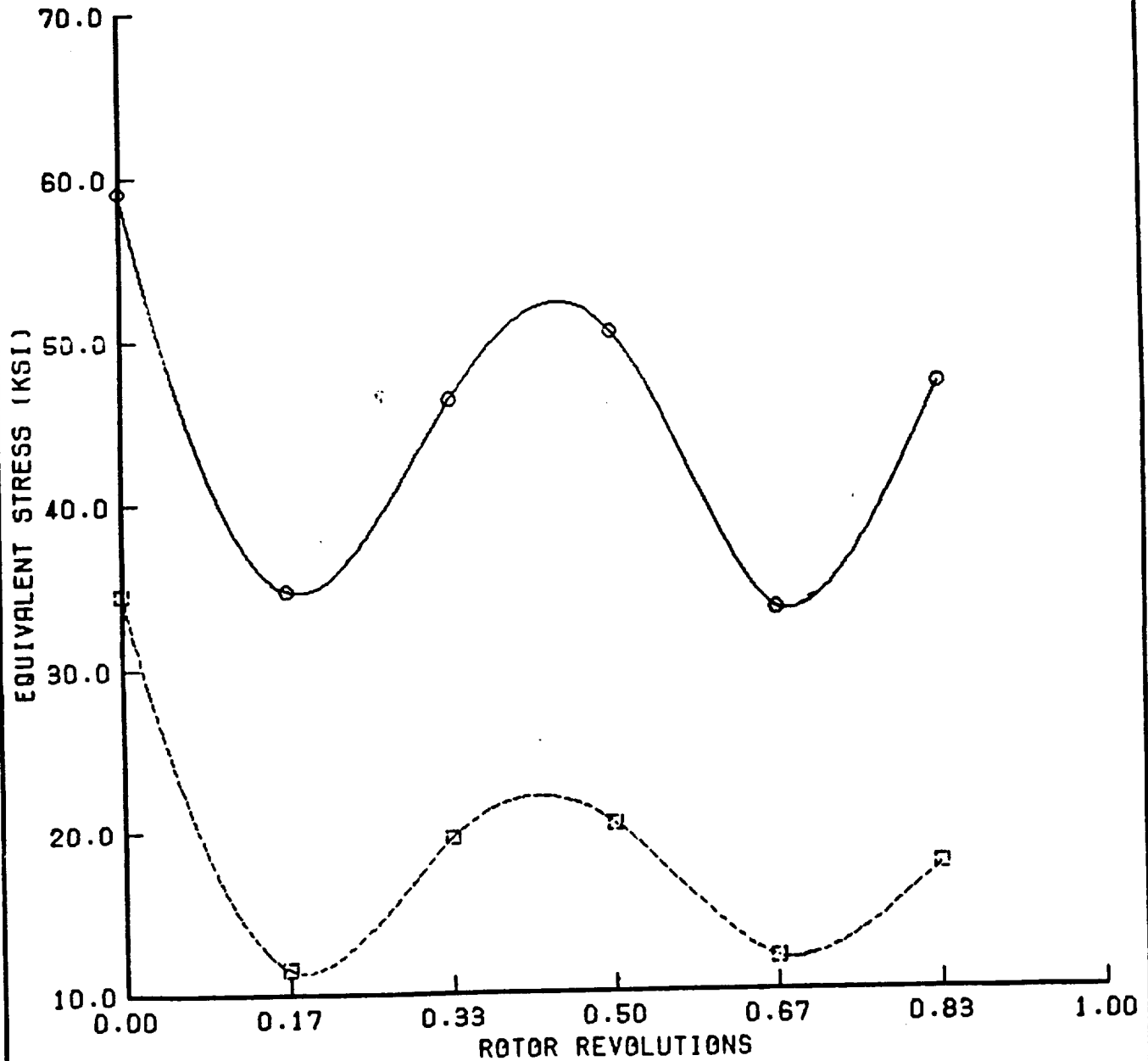


Figure 20. A Comparison of Critical Cyclic Stresses in SiC/Al and Stainless Steel Rotors

Table 5

A Comparison of Mean and Amplitude Stresses -
Shallow Pocket Rib

ROTOR MATERIAL	MEAN STRESS (KSI)	AMPLITUDE STRESS (KSI)
20 v/o SiC/AL-A201	23.2	11.4
17-4 ph Stainless Steel	46.6	12.5

In order to utilize the fatigue data obtained during the fatigue testing of the material, an equivalent fully reversed cyclic stress had to be approximated. The fatigue testing completed on SiC/AL specimens used a fully reversed cyclic stress ($\sigma_m=0$) to determine the fatigue life of the material. The actual stresses in the rotor cycled between a maximum and minimum level as shown in Figure 20, and do not have a mean stress equal to zero. Therefore, an equivalent amplitude stress (σ_{ae}) representing a completely reversed condition was approximated using methods outlined in Reference 25. These equivalent amplitude stresses for both rotor materials are listed below.

<u>ROTOR MATERIAL</u>	<u>EQUIVALENT AMPLITUDE STRESS (KSI)</u>
20 v/o SiC/Al-A201	21.6
17-4 ph Stainless Steel	23.0

Results

Static

The maximum static stress that the SiC/Al rotor experienced is 34.5 Ksi (Figure 20). This peak occurred in the critical shallow pocket rib area

when the rotor is in the TDC position. The temperature in that region ranges from 400-450°F. The results of the high temperature mechanical testing found that the yield strength of 20 v/o SiC/A201-T6 is approximately 35 Ksi at 450°F. These preliminary results indicate that the material does not provide any factor of safety in the static design of the rotor. However, it is important to note that: 1. the model used was a simplified shell model which was generated for a comparative analysis; 2. material testing did not show any increases in material strength that were expected and can possibly be obtained with further material development; and 3. the analytical model was based upon the design of a stainless steel rotor, which inherently has much higher strength than aluminum alloys. Redesigns of the rotor should lower peak stresses or temperatures in the critical areas.

Fatigue

The results of the factigue testing and fatigue analyses suggest a life of 100 million cycles for the SiC/Al rotor compared to an infinite life for the steel rotor. These predictions were based on the estimated values of equivalent completely reversed stresses and high temperature fatigue data. Based on continuous operation, at a crankshaft speed of 8000 RPM (rotor speed 2667 RPM) the predicted life of the SiC/Al rotor is 625 hours. It is anticipated that a life of 3000 hours is obtainable if peak stresses and temperatures could be lowered in a redesign and better definition can be obtained of the material's high temperature fatigue properties in the 100 to 500 million cycles testing range.

8.0 CONCLUSIONS AND RECOMMENDATIONS

8.1 Conclusions

The major conclusion is that, on the basis of the feasibility design study, cast SiC/Al appears to be a viable materials candidate for rotors of rotary engines. The result would be a substantial weight savings, approaching 17% of the total engine weight.

A more subjective conclusion, based on an assessment of material properties and component performance requirements, but unsupported by design and analysis studies, is that cast SiC/Al may be applicable to other components, primarily for the end housing and trochoid housing.

The cast SiC/A201-T6 material, as it currently stands in its development phase, appears reasonably adequate for component usage, as outlined above, without major materials refinements needed.

8.2 Recommendations

It is specifically recommended that NASA-Lewis, on the basis of the accomplishments of this Phase I study, support the development of a cast SiC/Al rotor program. Major elements of this program should include:

1. the design of a rotor specifically aimed at utilizing the properties of SiC/Al while maintaining current functionality requirements;
2. the conduct of additional mechanical testing of SiC/Al to acquire design and analysis critical information. Such information to include: high temperature fatigue resistance at 250 million cycles; creep behavior at high temperature; and wear resistance at high temperature;

3. an assessment of rotor fabricability using the cast SiC/Al material. Such assessment to include the fabrication of one or more SiC/Al rotors.

It is suggested to NASA and to John Deere Technologies that John Deere participate in this proposed program by assisting in the design of a cast SiC/Al rotor.

It is further recommended to Dural Aluminum Composites Corporation that refinements to their casting process be investigated to improve the properties of the baseline process and to improve the homogeneity and properties of this material.

9.0 REFERENCES

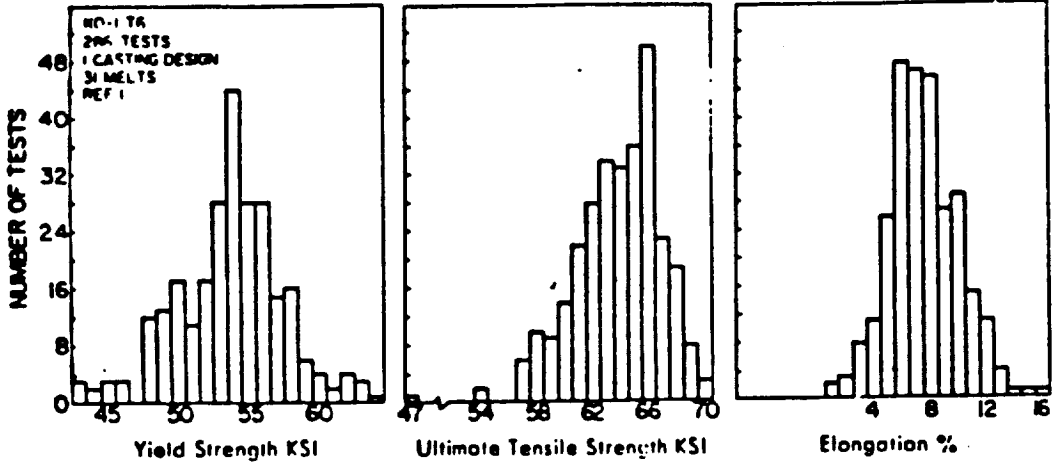
1. H.M. Stoller, "The Application of Cast SiC/Al to Rotary Engine Components", FY85 Phase I SBIR Proposal, Submitted by SANTECH, Inc. to NASA, May 23, 1985.*
2. D.M. Schuster, "Cast Discontinuously Reinforced SiC/Al", Presented at the 7th Annual Working Group Review Meeting on Discontinuous Reinforced Al Materials, Pack City, UT., January 1985. Also contained in sales literature prepared by Scientific Applications International Corporation, 1984.
3. D.L. McDanel and C.S. Hoffman, "Microstructure and Orientation Effects on Properties of Discontinuous Silicon Carbide/Aluminum Composites", NASA Technical Paper 2302, July 1984.
4. Personal Communication with Dr. D.M. Schuster, Report of Ford Motor Company Wear Tests, January 1985.
5. P. Badgley, et al, "Advanced Stratified Charge Rotary Aircraft Engine Design Study", NASA CR-165398, January 29, 1982.
6. Avco Specialty Materials Division, Silicon Carbide Composite Materials, Specification Literature.
7. DWA Composite Specialties, Inc., DWAL "20" Super Aluminum, Specification Literature.
8. ARCO, Metals Division, Silag Operations, Specification Literature.
9. "SAI Develops SiC/Al Casting Process", Current Highlights, DoD Metal Matrix Composites Information Analysis Center, V4, N3, September 1984.
10. "Casting Process Cuts Metal Matrix Price", Hi-Tech Materials Alert", Technical Insights, Inc., N8, August 1984.
11. Personal Examination of Photomicrographs. Materials provided by D.M. Schuster, September 1984.
12. R. Kamo and R.M. Kakwani, "Adiabatic Wankel Type Rotary Engine", Adiabatics, Inc., Phase I Final Report, NAS3-24535, June 1985.
13. H. Hamilton, L.M. Crain and E.L. Stanton, "PDA/PATRAN-G: A System for the Creation and Display of General Three-Dimensional Models", in Finite Element Systems, ed. C.A. Brebbia, Springer-Verlag, 1982, pp. 307-323.

* SANTECH, Inc. was subsequently acquired by PDA Engineering

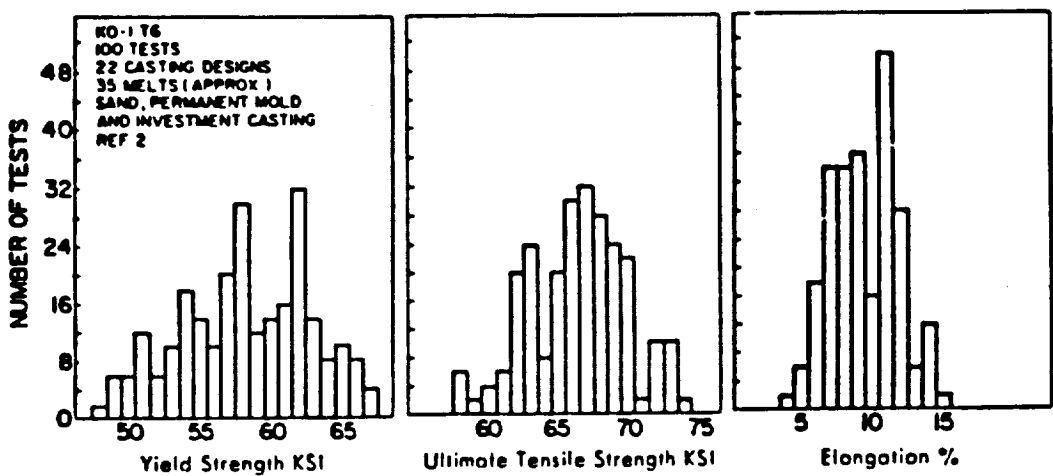
14. H.M. Stoller, et al, "The Application of Cast SiC/Al to Rotary Engine Components", PDA 86-MPR-5333-00-01 through -05, NAS 3-2487, March through July, 1986.
15. Personal communication with Dr. D.M. Schuster, July 1986.
16. "Metallic Materials and Elements for Aerospace Vehicle Structures", MIL-HDBK-5B, Vol. 1 (1971) Department of Defense, Washington, D.C.
17. "Metals Handbook", American Society for Metals, Metals Park, Ohio.
18. "Engineering Data for Aluminum Structures", Aluminum Construction Manual, Section 3, 3rd Edition (1975), The Aluminum Association Inc. New York N.Y.
19. K. Yamamoto, Rotary Engine, Sankaido, Co., Ltd., Tokyo, 1981.
20. Personal communication with John Deere Technologies.
21. C. Jones, U.S. Patent 3,230,787, January 25, 1966 and M. Bentele, et al, U.S. Patent 3,111,261, November 19, 1963.
22. Personal communication with Charles Jones, John Deere Technologies.
23. "Rotor, 7.5:1 Compression Ratio Drawing 21002N", Curtis Wright Corp., 6 June 1983.
24. "ANSYS Computer Program", Revision 4.2, Swanson Analysis Systems, Inc., 1985.
25. R.G. Budynas, Advanced Strength and Applied Stress Analysis, McGraw-Hill Book Co., 1977.

APPENDIX A

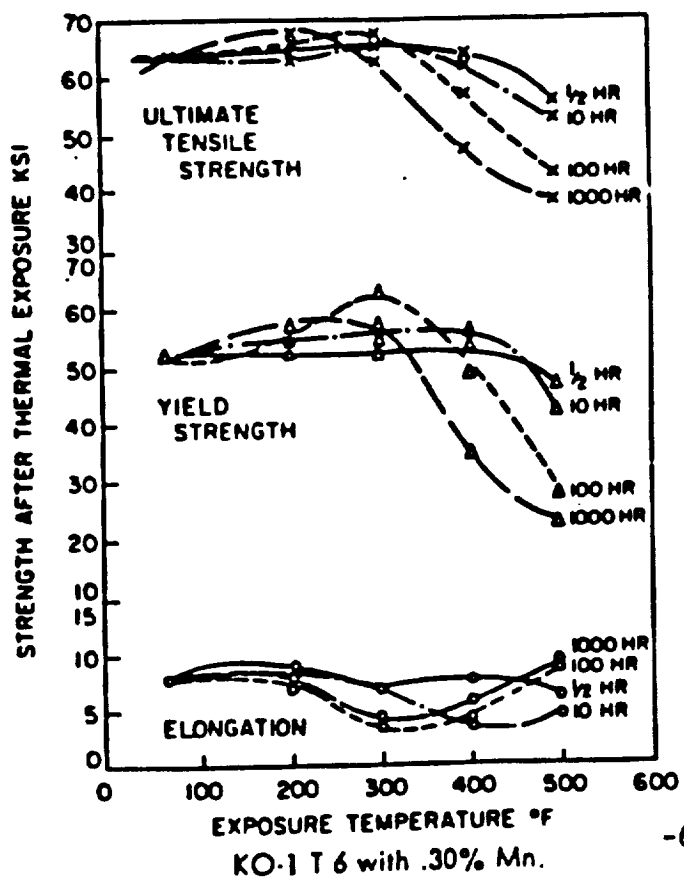
MANUFACTURER'S MECHANICAL PROPERTIES
DATA ON A201-T6



(a) Property variations realized in sand cast test spar castings having sections from 1/4" to 3". (Cast 1966).



(b) Property variations realized on a wide variety of castings and casting processes. (Cast 1964 through 1968).



A201-T6 Reference Data

From Conalco Technical Information Report CDRL-75-TIR-3, Composition, Properties, and Metallography of Casting Alloy 201.

ORIGINAL PAGE IS OF POOR QUALITY

1 September 1971

Table A1. *Design Mechanical and Physical Properties for 201.0 Aluminum Alloy (castings)*

Specification	AMS 4228		AMS 4229	
	Castings		Castings	
Form	T6		T7	
Temper	T6		T7	
Class ^d	1 ^b	10 ^c	2 ^b	11 ^c
Basis	S	S	S	S
Mechanical Properties:				
F_{Tu} , ksi	60	56	60	56
F_{Ty} , ksi	50	48	50	48
F_{Cy} , ksi	51	49	-	-
F_{Su} , ksi	37	35	-	-
F_{bry} , ksi:				
(e/D = 1.5)	90	84	-	-
(e/D = 2.0)	115	107	-	-
F_{bry} , ksi:				
(e/D = 1.5)	77	74	-	-
(e/D = 2.0)	90	86	-	-
ϵ , percent:				
in 2 in. or 4D	5	3	3	1.5
E , 10^3 ksi		10.3		
E_c , 10^3 ksi		10.7		
G , 10^3 ksi		4.0		
μ		0.33		
Physical Properties:				
ω , lb/in. ³		0.101		
C , Btu/(lb)(F)		0.22 (at 212 F)		
K , Btu/[(hr)(ft ²)(F)/(ft)]		70. (at 77 F)		
α , 10^{-6} in./in./F		(See Figure 3.12.1.0)		

^dClass designations are defined in MIL-A-21180C.

^bProperties in Classes 1 and 2 are obtainable only in designated areas within casting.

^cProperties in Classes 10 and 11 apply to unspecified locations within casting.

A201-T6 Reference Data

From MIL-HDBK-5B, 1 September 1971,
Metallic Materials and Elements for
Aerospace Vehicle Structures.

APPENDIX B

HIGH TEMPERATURE MODULUS DATA

A201-T6 CAST ALUMINUM (HIPPED)
AVERAGE YOUNG'S MODULUS VS. TEMPERATURE

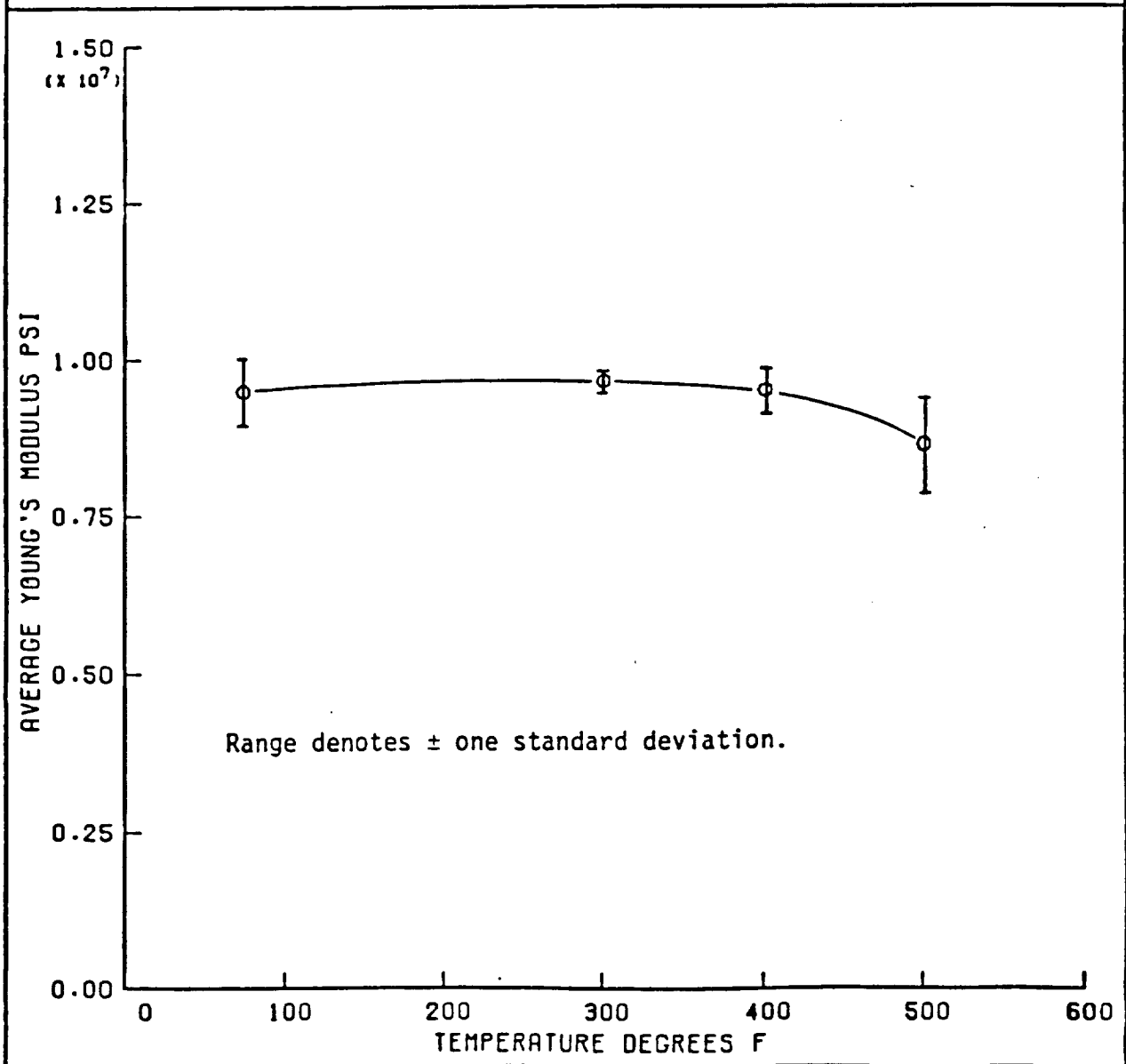


Figure B-1

10% SILICON CARBIDE / ALUMINUM
AVERAGE YOUNG'S MODULUS VS. TEMPERATURE

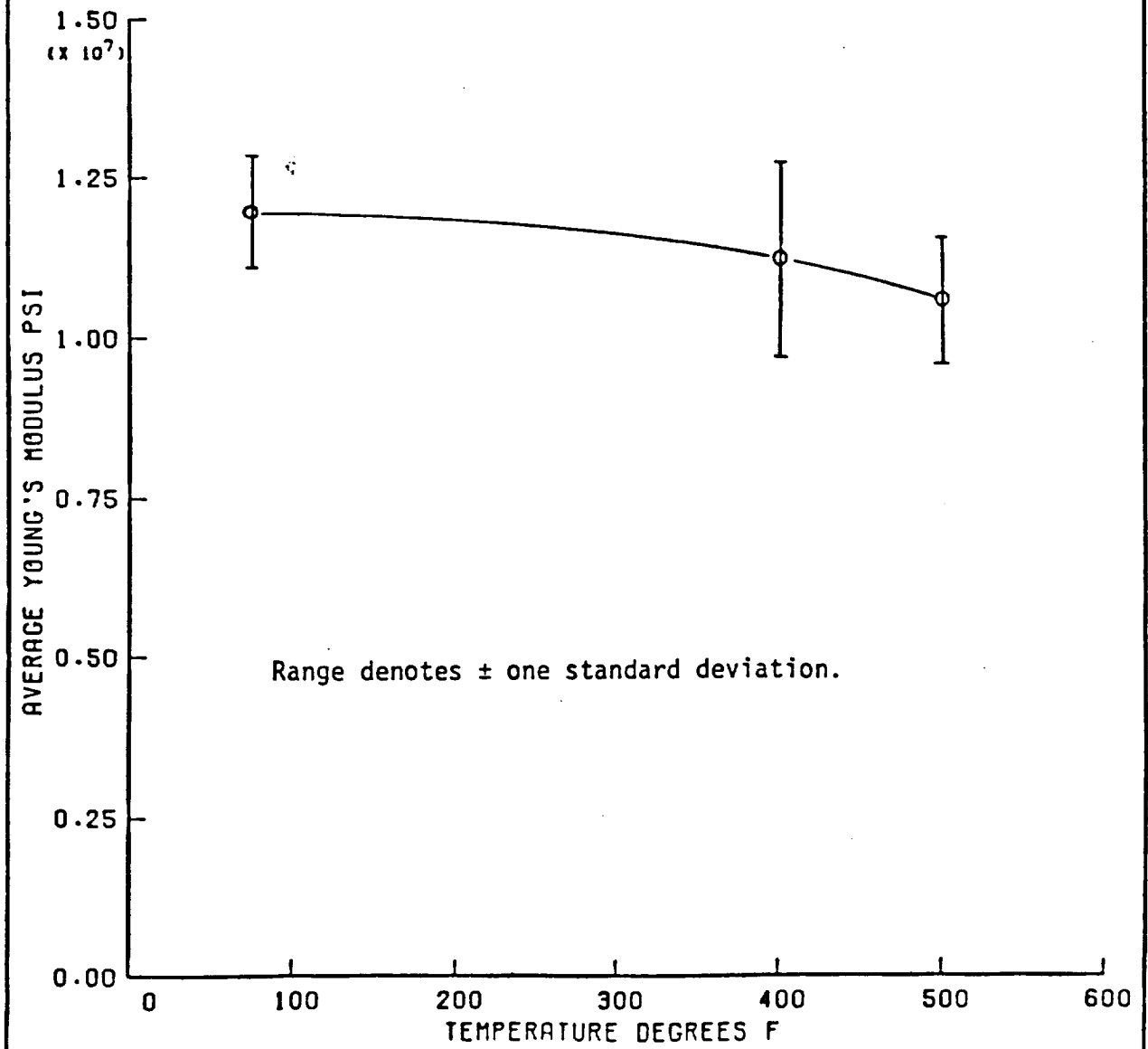


Figure B-2
-65-

20V% SILICON CARBIDE / ALUMINUM
AVERAGE YOUNG'S MODULUS VS. TEMPERATURE

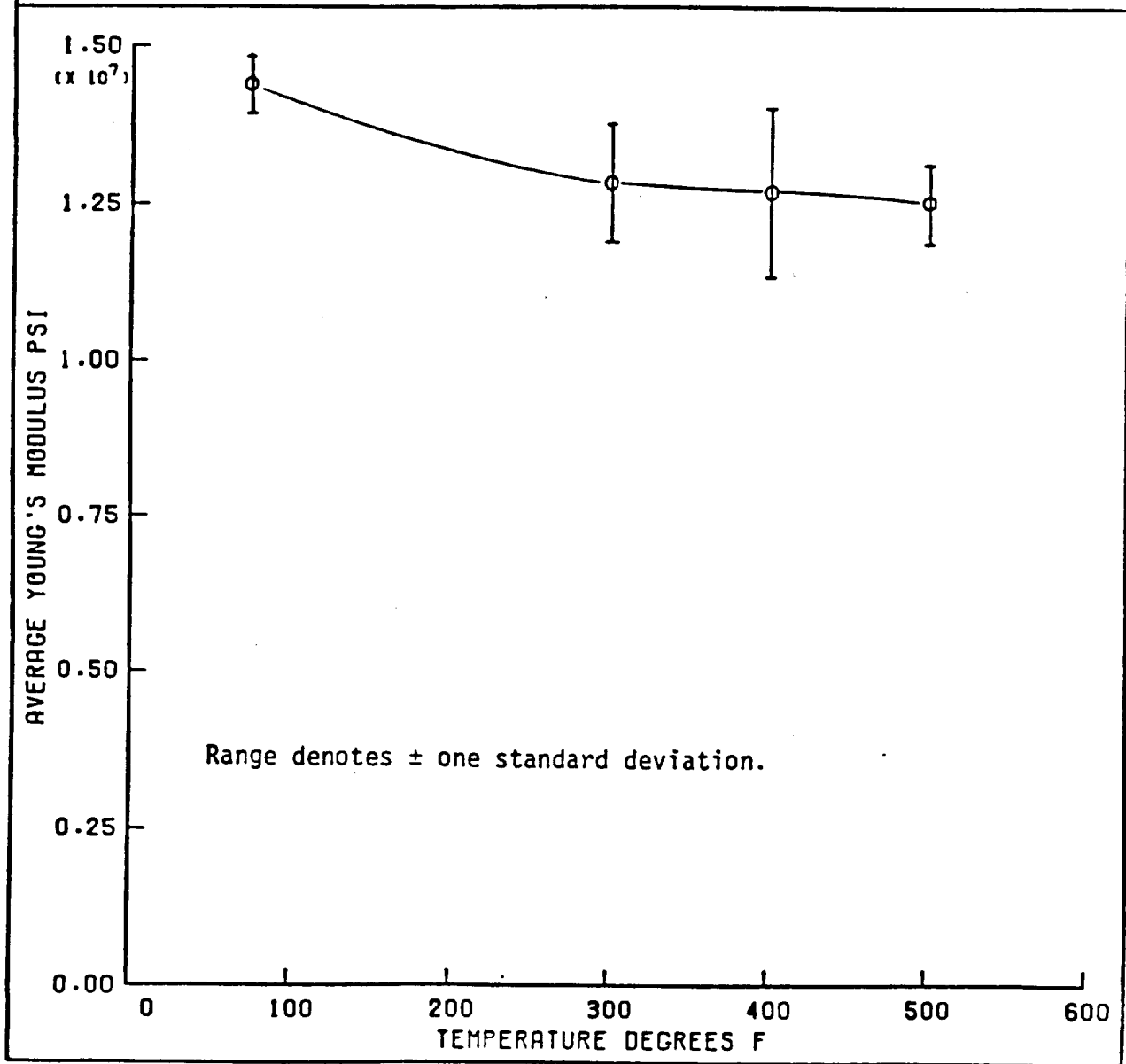


Figure B-3

A201-T6 CAST ALUMINUM (HIPPED)
YOUNG'S MODULUS VS. TEMPERATURE

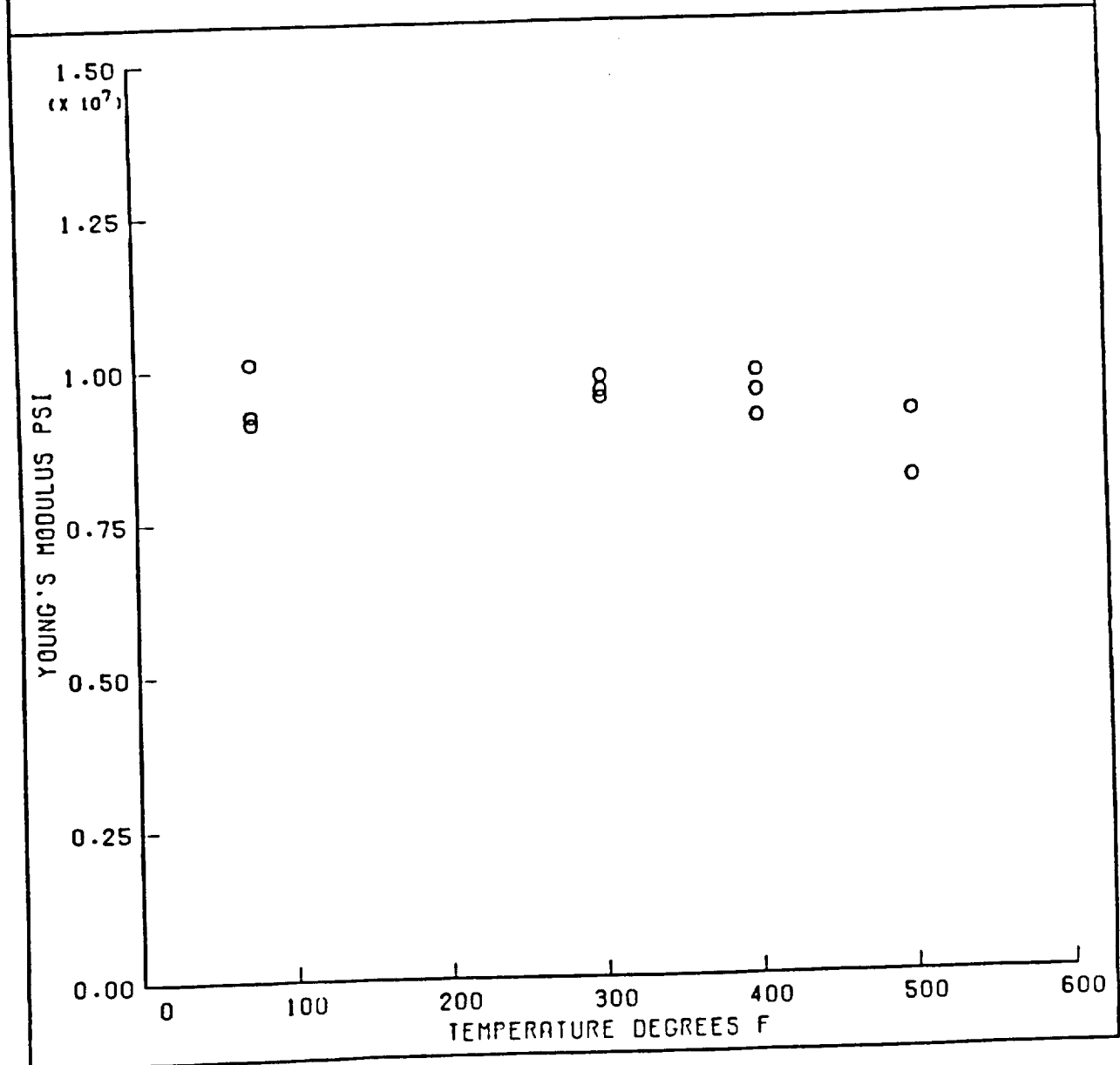


Figure B-4
-67-

10% SILICON CARBIDE / ALUMINUM
YOUNG'S MODULUS VS. TEMPERATURE

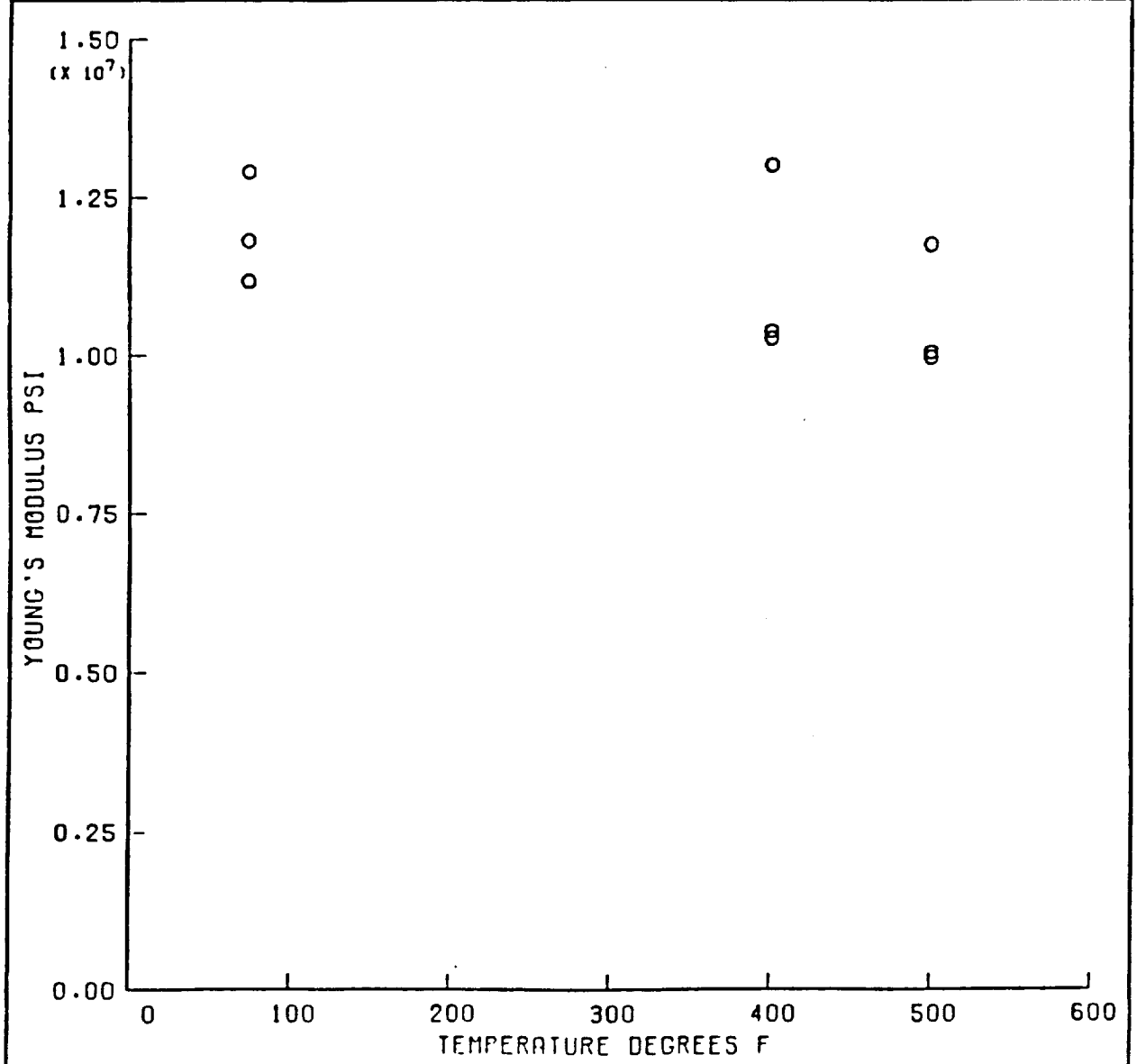


Figure B-5
-68-

20V% SILICON CARBIDE / ALUMINUM
YOUNG'S MODULUS VS. TEMPERATURE

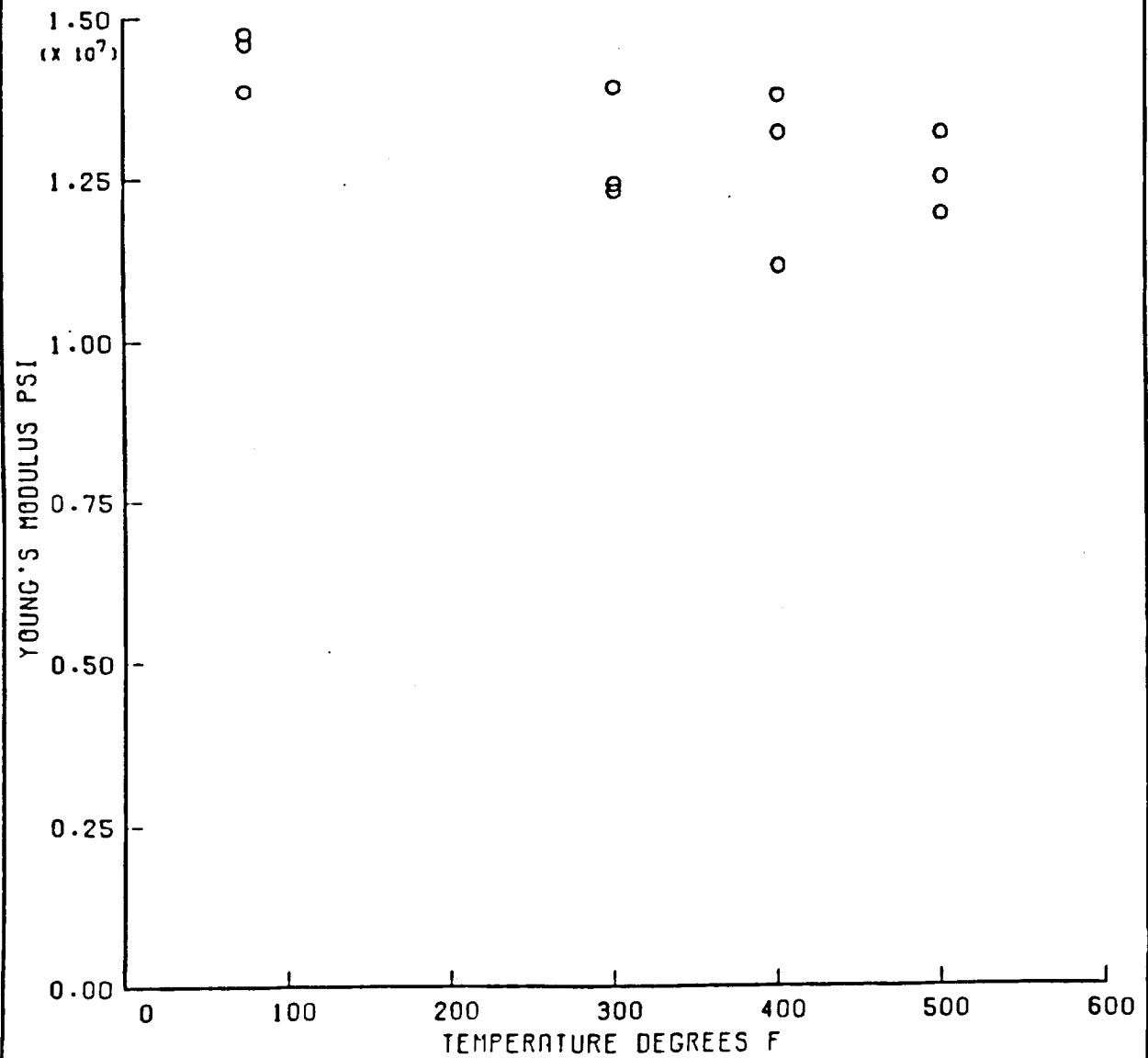
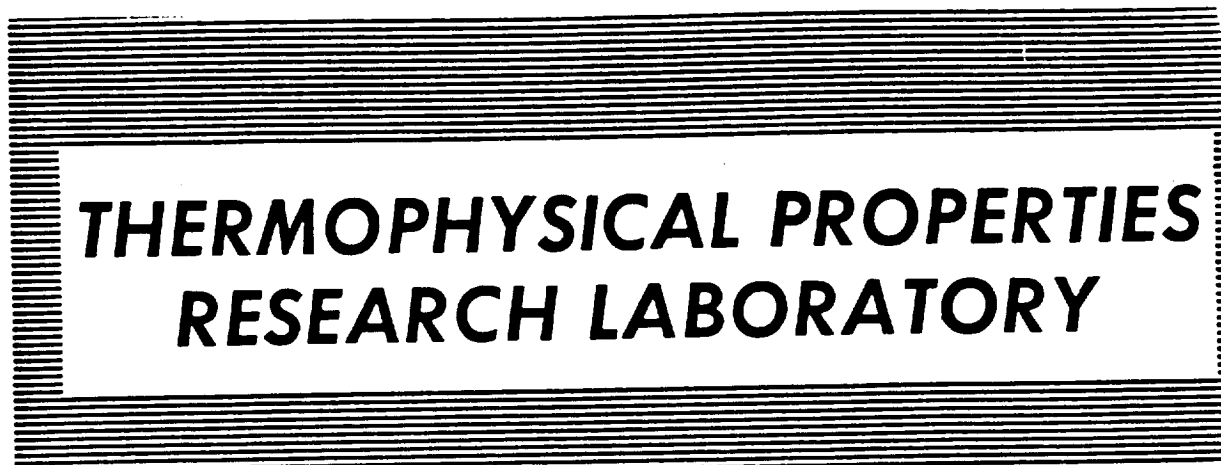



Figure B-6
-69-

APPENDIX C

THERMAL CONDUCTIVITY OF 10 v/o and 20 v/o SiC/A201-T6



**THERMOPHYSICAL PROPERTIES
RESEARCH LABORATORY**

TPRL 521

Thermal Conductivity of SiC/Al
(A Report to PDA Engineering)

by

R. E. Taylor, H. Groot and J. Larimore

April 1986

School of Mechanical Engineering
Purdue University, West Lafayette, Indiana

TPRL 521

Thermal Conductivity of SiC/Al

(A Report to PDA Engineering)

by

R. E. Taylor, H. Groot and J. Larimore

April 1986

TABLE OF CONTENTS

	Page
INTRODUCTION	1
RESULTS AND DISCUSSION	2

LIST OF TABLES

1. Sample Geometries and Bulk Density Values.	4
2. Specific Heat Results.	4
3. Thermal Diffusivity Results.	5
4. Thermal Conductivity Calculations	5

LIST OF FIGURES

1. Differential Scanning Calorimeter.	6
2. Digital Data Acquisition System.	7
3. Flash Diffusivity Apparatus.	8
4. Specific Heat.	9
5. Thermal Diffusivity.	10
6. Thermal Conductivity	11

Thermal Conductivity of SiC/Al

INTRODUCTION

Two samples of SiC dispersed in an aluminum matrix were submitted by J. Norman of PDA Engineering for thermal conductivity testing. One sample contained 10 volume percent of SiC (10V) and the other contained 20 volume percent (20V). The bulk density (d), specific heat (C_p) and thermal diffusivity (α) were measured. The thermal conductivity (λ) was calculated as the product of these quantities, i.e. $\lambda = \alpha C_p d$.

Specific heat was measured using a standard Perkin-Elmer Model DSC-2 Differential Scanning Calorimeter (Figure 1) using sapphire as a reference material. The standard and sample, both encapsulated in pans, were subjected to the same heat flux and the differential power required to heat the sample at the same rate was recorded using the digital data acquisition system (Figure 2). From the mass of the sapphire standard, pans, the differential power, and the known specific heat of sapphire, the specific heat of the sample is computed. The experimental data is visually displayed as the experiment progresses. All measured quantities are directly traceable to NBS standards.

Thermal diffusivity was determined using the laser flash diffusivity method. The flash method, in which the front face of a small disc-shaped sample is subjected to a short laser burst and the resulting rear face temperature rise is recorded, is used in over 80% of the present thermal diffusivity measurements throughout the world. A highly developed apparatus

exists at TPRL (Figure 3) and we have been involved in an extensive program to evaluate the technique and broaden its uses. The apparatus consists of a Korad K2 laser, a high vacuum system including a bell jar with windows for viewing the sample, a tantalum tube heater surrounding a sample holding assembly, a spring-loaded thermocouple or an i.r. detector, appropriate biasing circuits, amplifiers, A-D converters, crystal clocks and a minicomputer based digital data acquisition system (Figure 2) capable of accurately taking data in the 40 microsecond and longer time domain. The computer controls the experiment, collects the data, calculates the results and compares the raw data with the theoretical model.

RESULTS AND DISCUSSION

The diffusivity sample dimensions, masses and bulk density values are given in Table 1. The bulk density of the 20V sample is only about one percent greater than that of the 10V sample.

Specific heat results are given in Table 2 and are plotted in Figure 4. The samples were rerun because of the relatively large "peak" and "valley" exhibited during initial heating. The peak and valley were evident for both samples. Results obtained during the reruns (after the samples had been heated to 317C) followed the normal pattern for annealed materials. It is not unusual for aluminum based materials to exhibit anomalies until they are annealed.

Thermal diffusivity results are given in Table 3 and are plotted in Figure 5. These measurements were made at selected temperatures and the samples were allowed to come to equilibrium before the laser pulse. The results for the two materials are fairly close to each other. The maximum difference is less than 8% and occur at the highest temperature measured.

Thermal conductivity values are calculated in Table 4. The annealed values are used for specific heat since the diffusivity results are obtained during conditions in which the anomalous specific heat behavior would not be a factor. The conductivity results are plotted in Figure 6. Because the diffusivity, specific heat and density values for the two materials are all similar, the conductivity values are also close together. The maximum difference is less than six percent.

ORIGINAL PAGE IS
OF POOR QUALITY

TABLE C1

Sample Geometries and Bulk Density Values

Sample Designation	Thick (in.)	Diameter (in.)	Mass (gms)	Density (gm cm ⁻³)
10V	0.201	0.5080	1.8882	2.828
20V	0.204	0.5060	1.9139	2.851

TABLE C2

Specific Heat Results

Temp. (C)	10V-RUN 1 (ws gm ⁻¹ K ⁻¹)	10V-RUN 2 (ws gm ⁻¹ K ⁻¹)	20V-RUN 1 (ws gm ⁻¹ K ⁻¹)	20V-RUN 2 (ws gm ⁻¹ K ⁻¹)
52.	0.9068	0.8937	0.8854	0.8755
77.	0.9351	0.9109	0.9280	0.9003
102.	0.9650	0.9332	0.9727	0.9270
127.	0.9866	0.9546	1.0034	0.9510
152.	1.0118	0.9729	1.0175	0.9712
162.	1.0247	0.9792	1.0178	0.9783
172.	1.0410	0.9843	1.0182	0.9840
182.	1.0623	0.9890	1.0241	0.9890
192.	1.0874	0.9930	1.0341	0.9929
202.	1.1068	0.9959	1.0333	0.9959
212.	1.1013	0.9983	1.0117	0.9983
222.	1.0570	0.9999	0.9759	0.9996
232.	0.9876	1.0003	0.9434	0.9999
242.	0.9050	1.0004	0.9088	1.0002
252.	0.8370	1.0006	0.8669	1.0016
262.	0.7956	1.0027	0.8259	1.0055
272.	0.7861	1.0095	0.8213	1.0142
282.	0.8219	1.0238	0.8761	1.0301
292.	0.8833	1.0466	0.9563	1.0518
302.	0.9446	1.0724	1.0233	1.0728
312.	1.0012	1.0956	1.0615	1.0897
317.	1.0219	1.1045	1.0728	1.0959

TABLE C3

Thermal Diffusivity Results

Sample Designation	Temp. (°C)	Diffusivity (cm ² sec ⁻¹)
10V	23	0.620
	75	0.582
	150	0.572
	225	0.597
	315	0.633
20V	23	0.627
	75	0.588
	150	0.597
	225	0.588
	315	0.588

TABLE C4

Thermal Conductivity Calculations

Sample Designation	Temp. (°C)	Density (gm cm ⁻³)	Specific Heat (Ws gm ⁻¹ K ⁻¹)	Diffusivity (cm ² sec ⁻¹)	Conductivity (Wcm ⁻¹ K ⁻¹)
10V	23	2.828	0.875	0.620	1.534
	75	2.828	0.910	0.582	1.498
	150	2.820	0.967	0.577	1.578
	225	2.828	1.000	0.597	1.688
	315	2.828	1.096	0.630	1.953
20V	23	2.851	0.855	0.627	1.528
	75	2.851	0.902	0.588	1.512
	150	2.851	0.967	0.591	1.629
	225	2.851	1.000	0.588	1.676
	315	2.851	1.098	0.588	1.841

ORIGINAL PAGE
BLACK AND WHITE PHOTOGRAPH

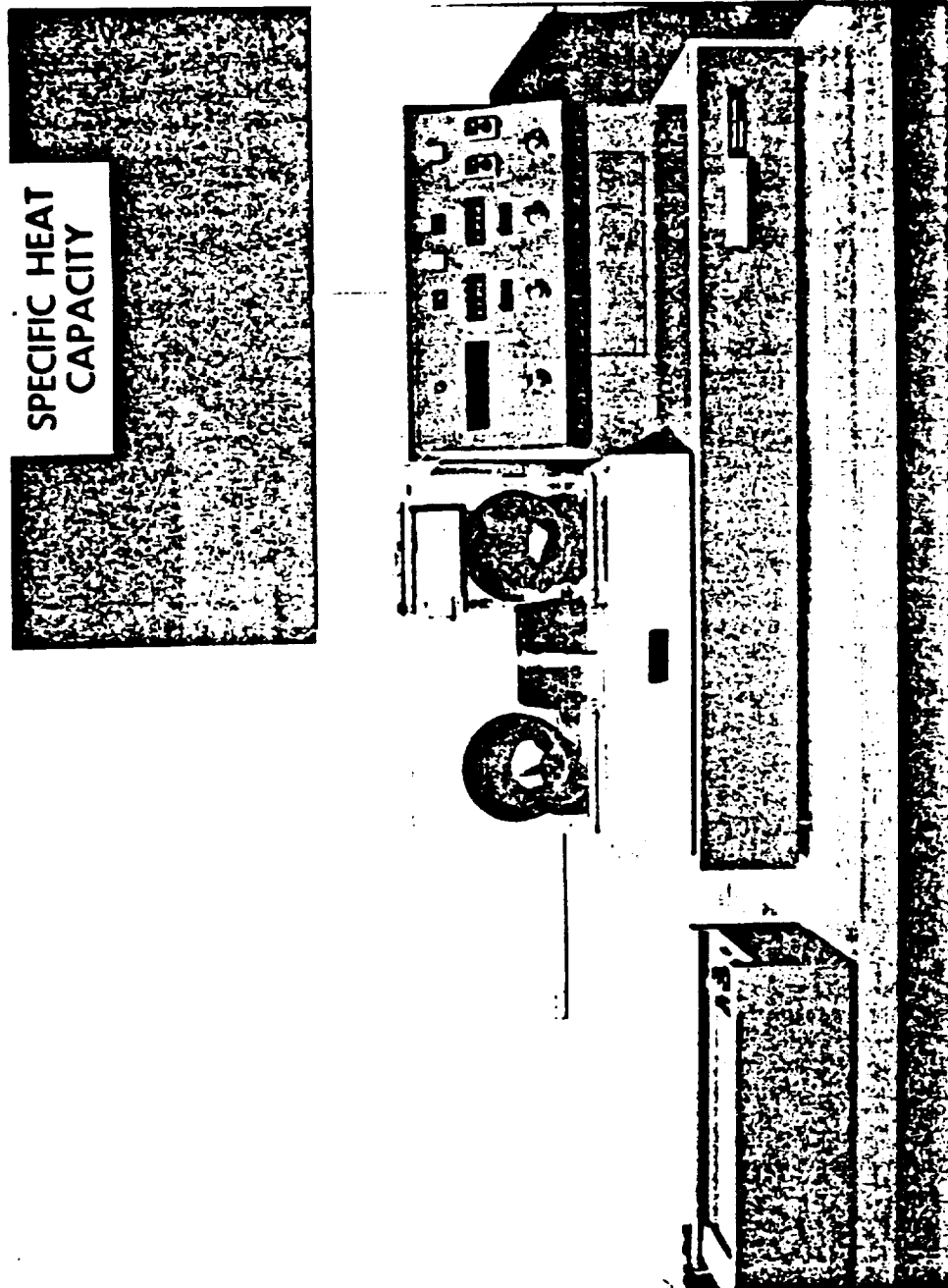


Figure C1 Differential Scanning Calorimeter

ORIGINAL PAGE
BLACK AND WHITE PHOTOGRAPH

ORIGINAL PAGE
BLACK AND WHITE PHOTOGRAPH

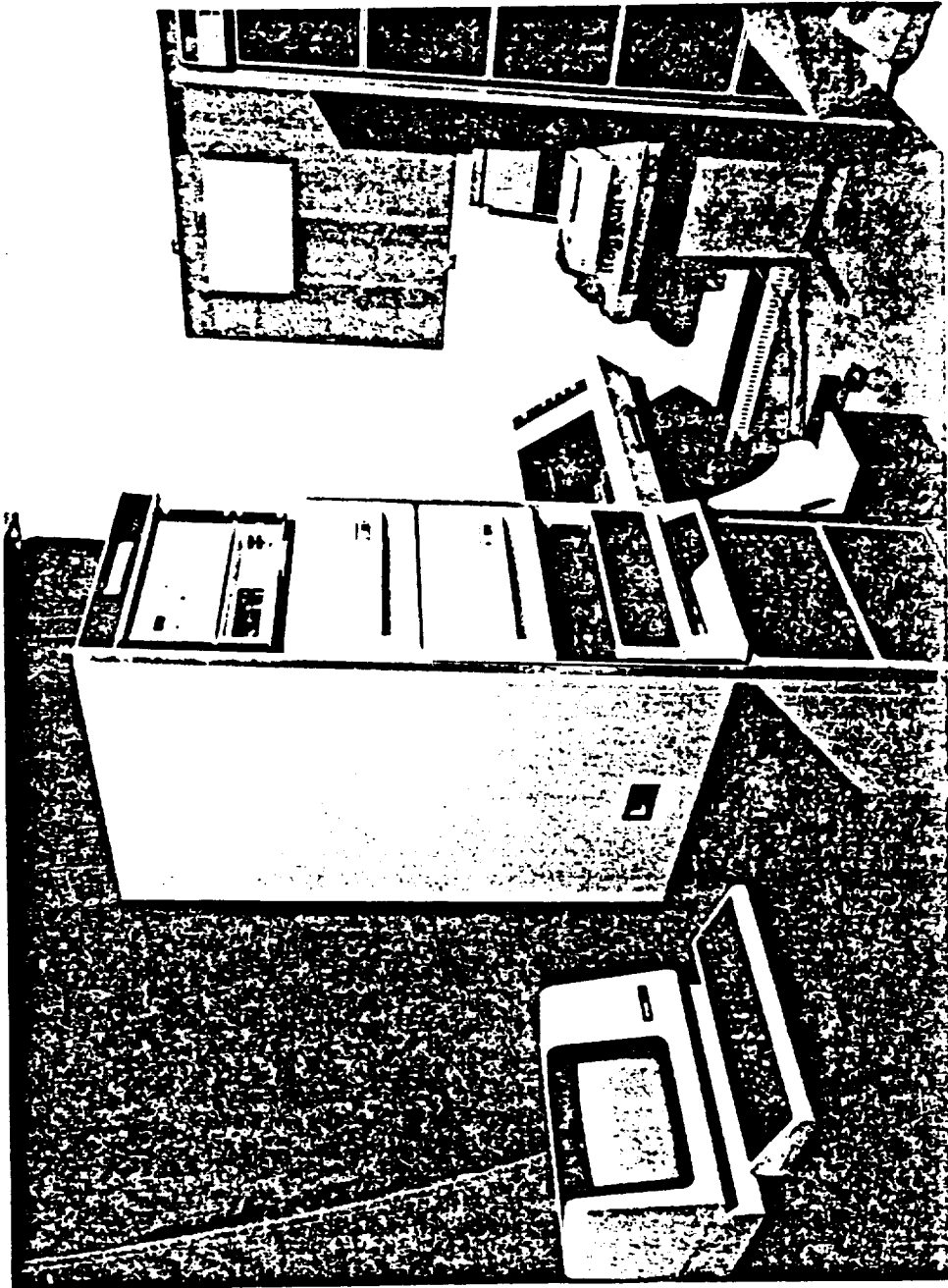


Figure C2 Digital Data Acquisition System

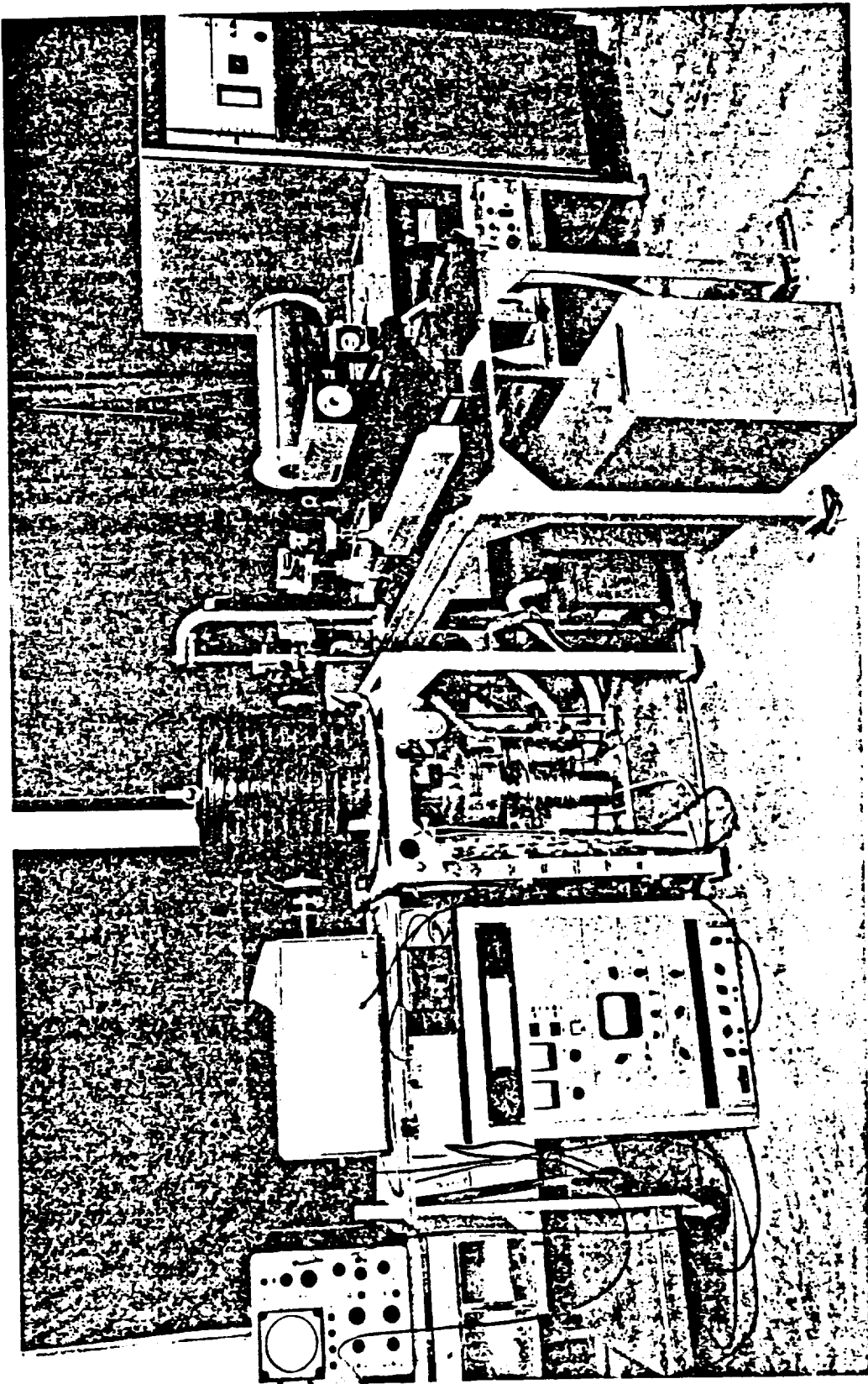


Figure C3 Flash Diffusivity Apparatus

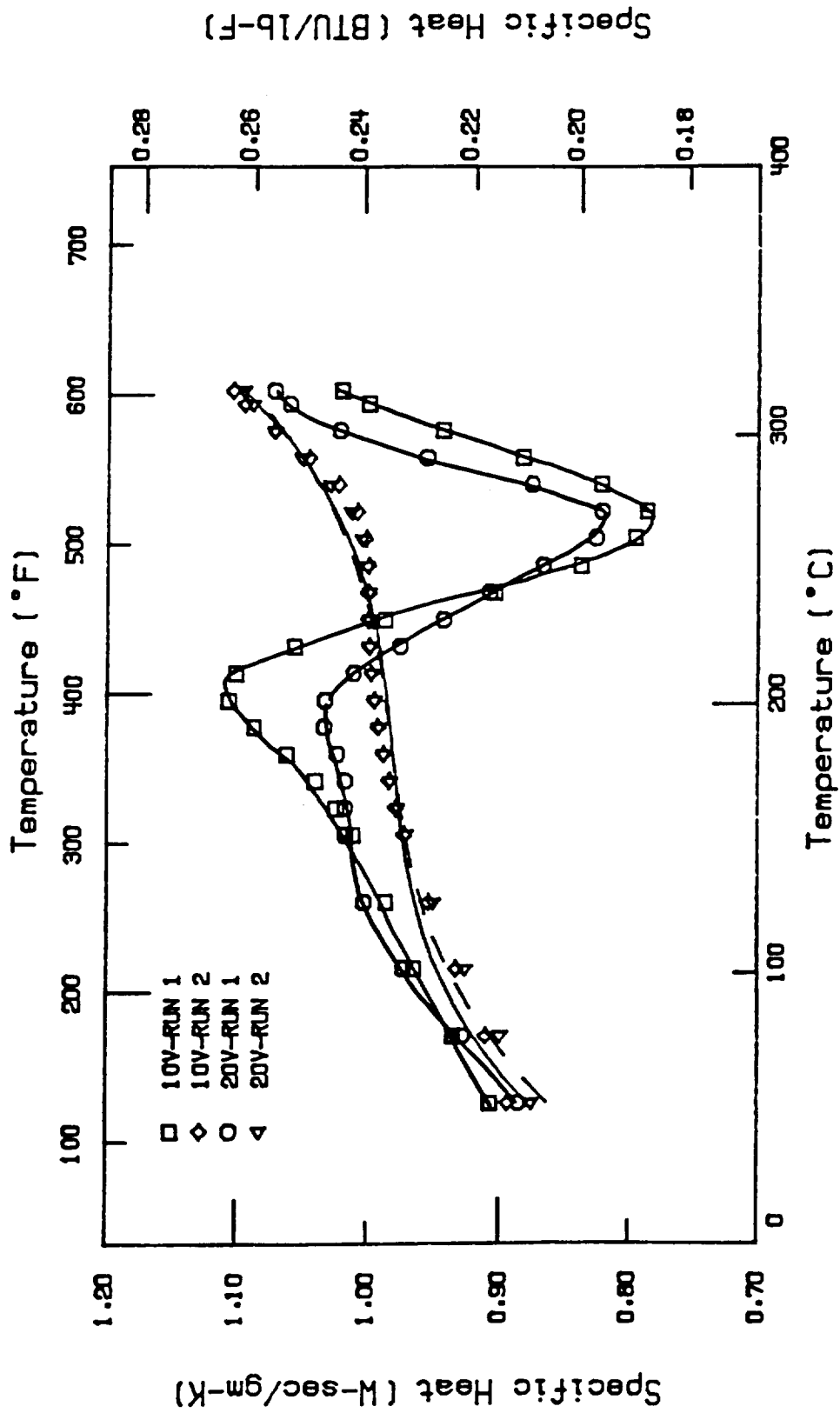


Figure C4 Specific Heat

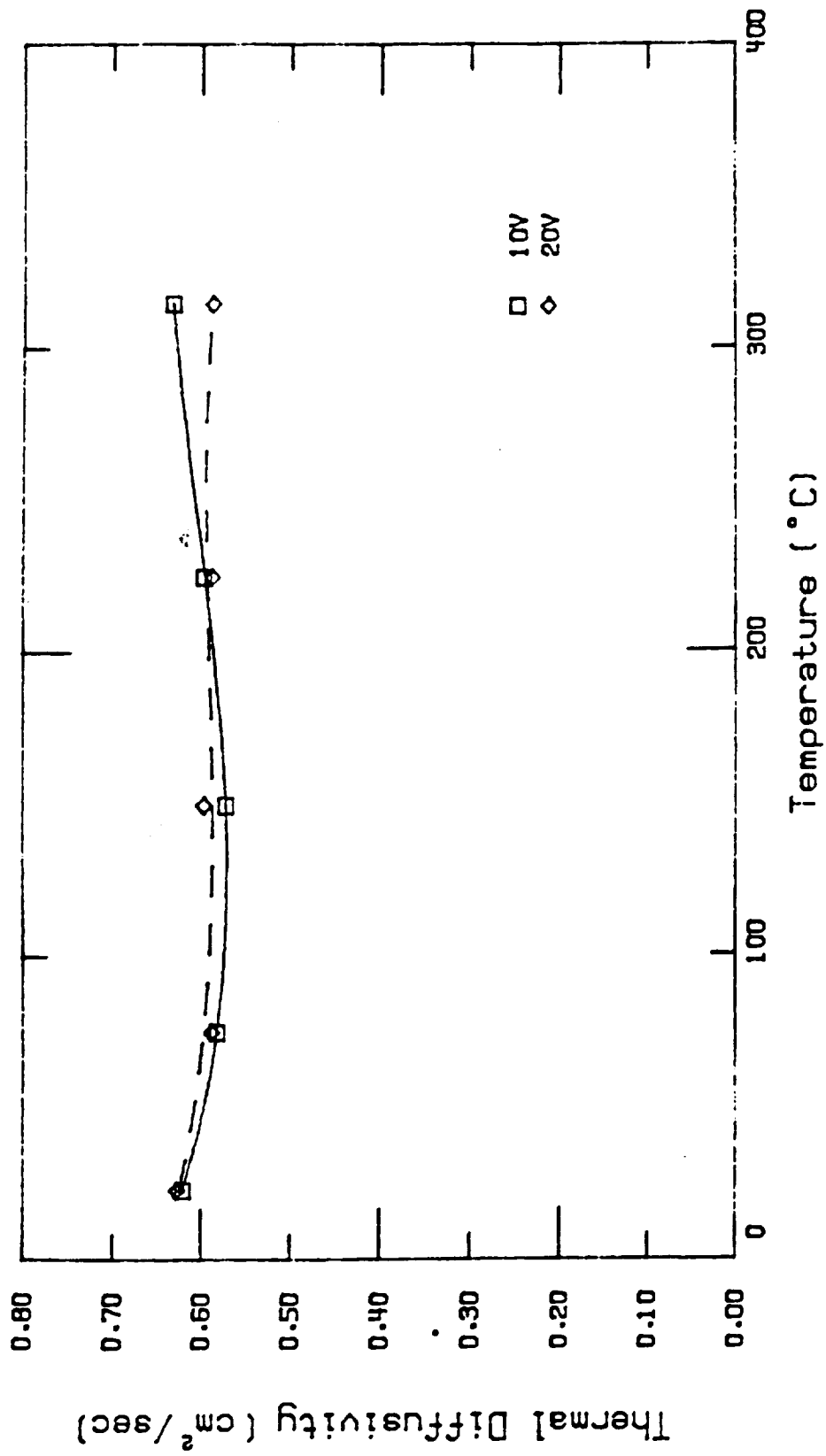


Figure C5 Thermal Diffusivity

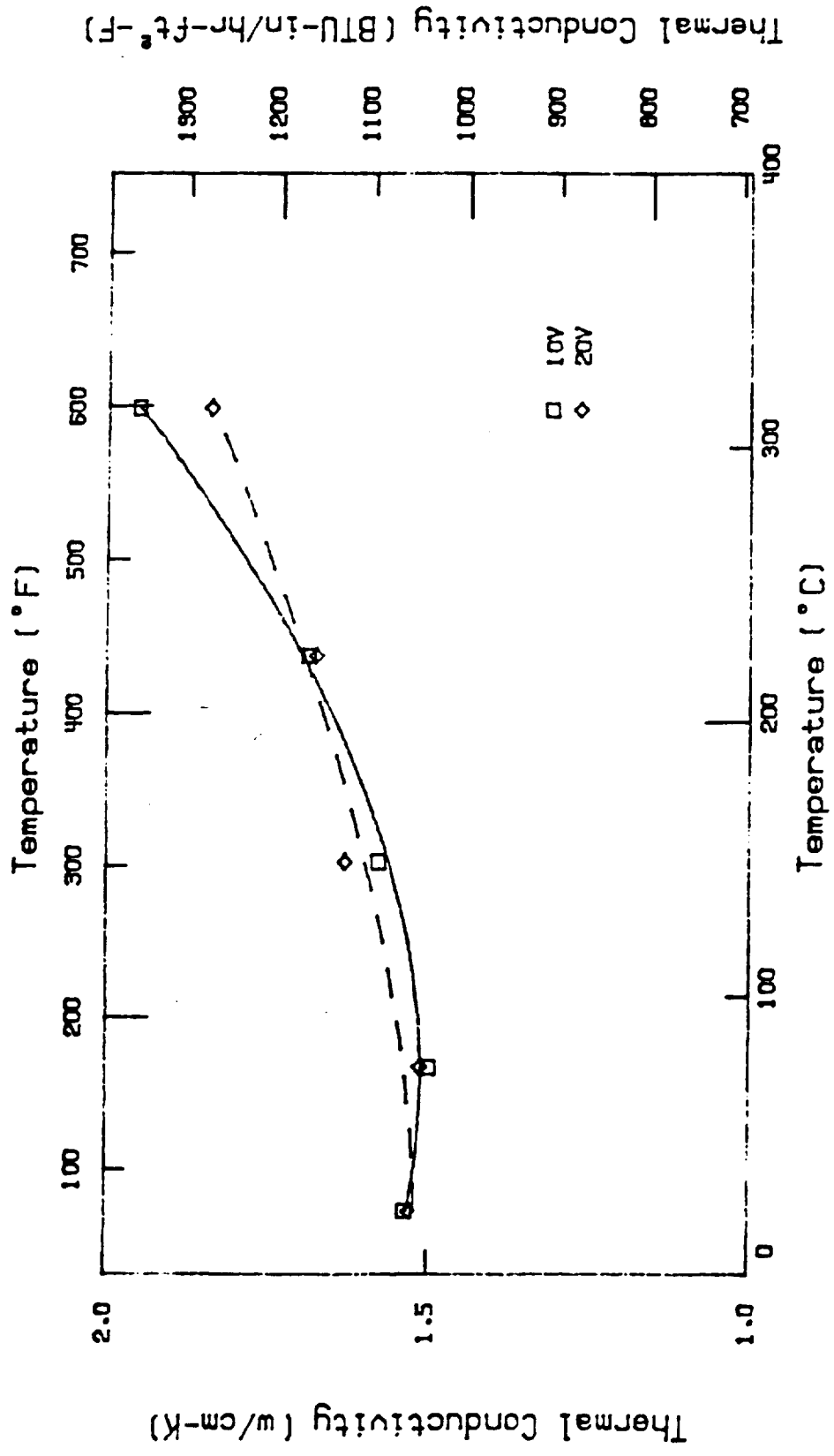


Figure C6 Thermal Conductivity

APPENDIX D

THERMAL EXPANSION OF 10 v/o and 20 v/o SiC/A201-T6

Coefficient of thermal expansion results from Analytical Services Corporation, Irvine, CA, using a Perkin-Elmer TMS-2 with Thermal Analysis Data Station.

<u>Specimen I.D.</u>	<u>Material</u>
201-2	A201-T6 (unhipped)
10V/0-2	10V/0 SiC/A201-T6 (hipped)
20V/0-2	20V/0 SiC/A201-T6 (hipped)

0.050

PDA ENG. 201-2

DIMENSION: 5.110 mm

LOAD: 0.000 g

SCAN RATE: 10.00 deg/min

FROM: 50

TO: 100

COEFF: 1.91E-05

FROM: 100

TO: 200

COEFF: 2.48E-05

FROM: 200

TO: 300

COEFF: 3.03E-05

MM

0.025

-87-

EXPANSION

0.000

50.00

80.00

110.00

140.00

170.00

200.00

230.00

260.00

290.00

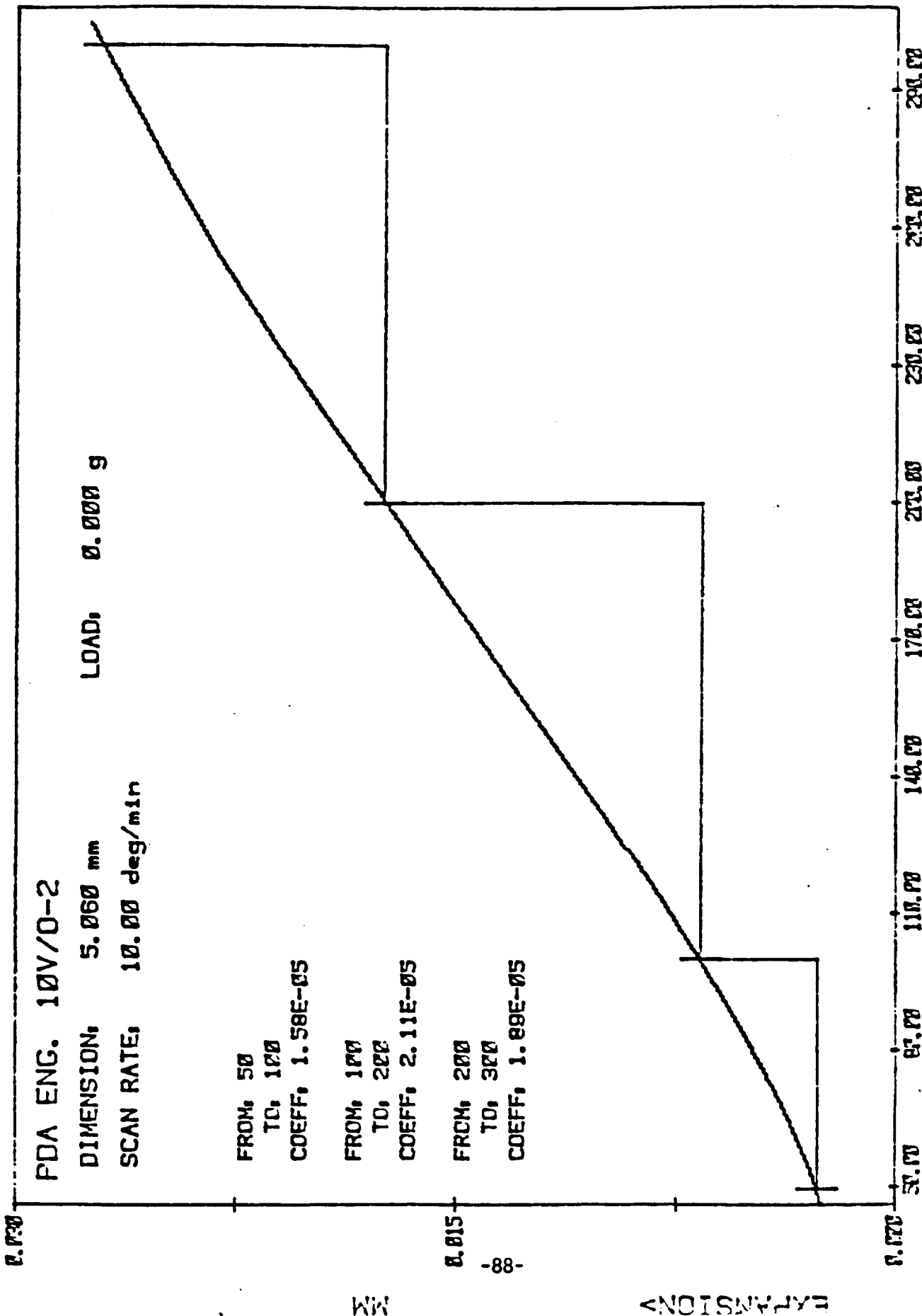
TMA

TEMPERATURE (C)

A. THOMAS FILE: 2012.7M

DATE: 04/15/RR TIME: 08:40

ORIGINAL PAGE IS
OF POOR QUALITY



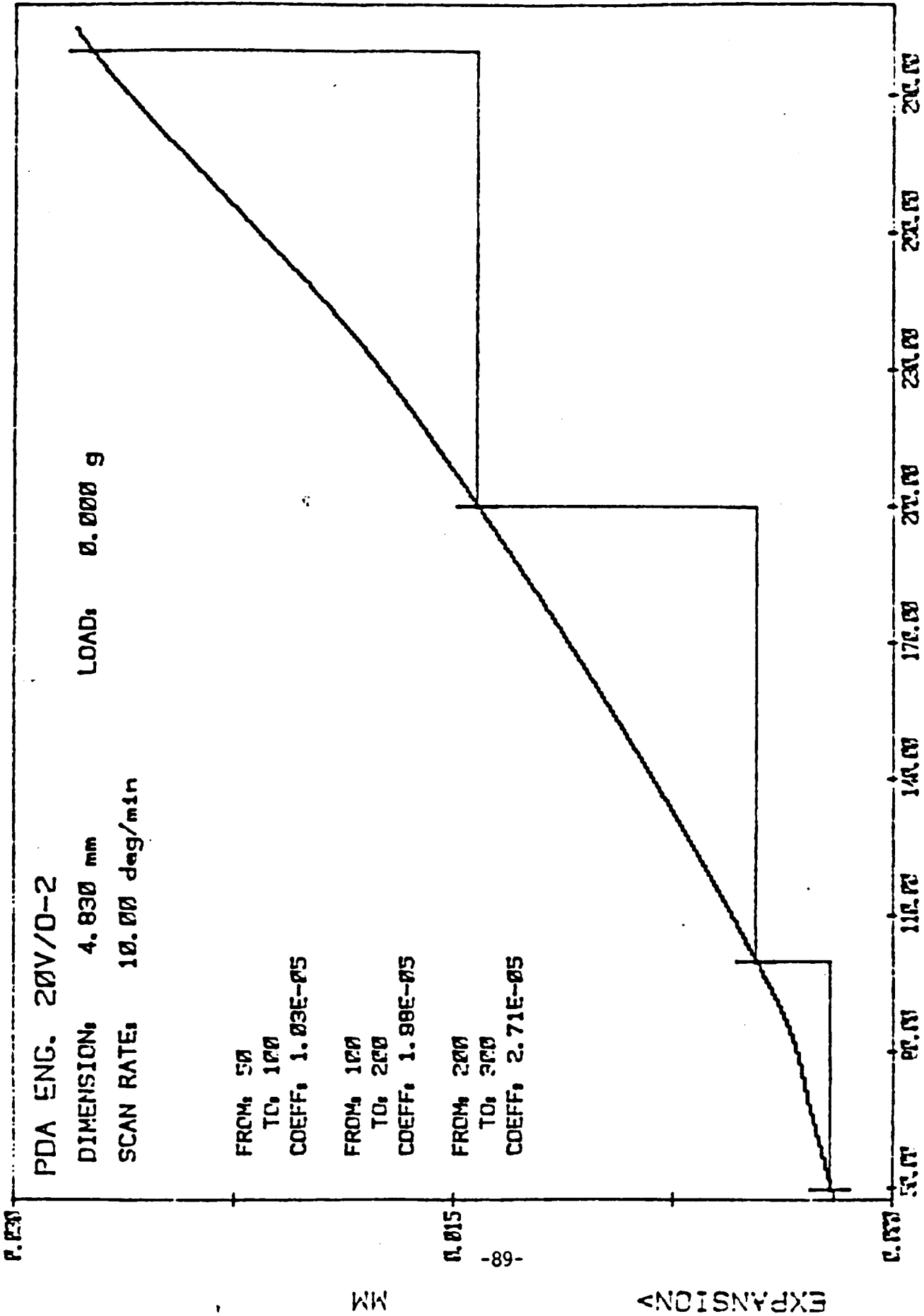
TMA

TEMPERATURE (C)

A. THOMAS FILE: 10V02. TM

DATE: 04/15/86 TIME: 10, 10

ORIGINAL PAGE IS
OF POOR QUALITY



TMA

TEMPERATURE (C)

A. THOMAS FILE: 20V.O-2

DATE: 04/14/86 TIME: 15:21

RESULTS:

Linear expansion coefficients - ppm/'C ; (ppm/'F)

Sample ID	Temperature ranges		
	50-100'C (122-212'F)	100-200'C (212-392'F)	200-300'C (392-572'F)
A201-T-6	18.1 (10.1)	23.4 (13.0)	25.8 (14.3)
20%	18.6 (10.3)	24.8 (13.8)	24.2 (13.4)
10%	15.6 (8.67)	17 (9.44)	20.9 (11.6)

ENCLOSURES:

Thermographs depicting linear displacement as a function of temperature are enclosed for each sample. CTE calculations, in ppm/'C, are included with thermographs.

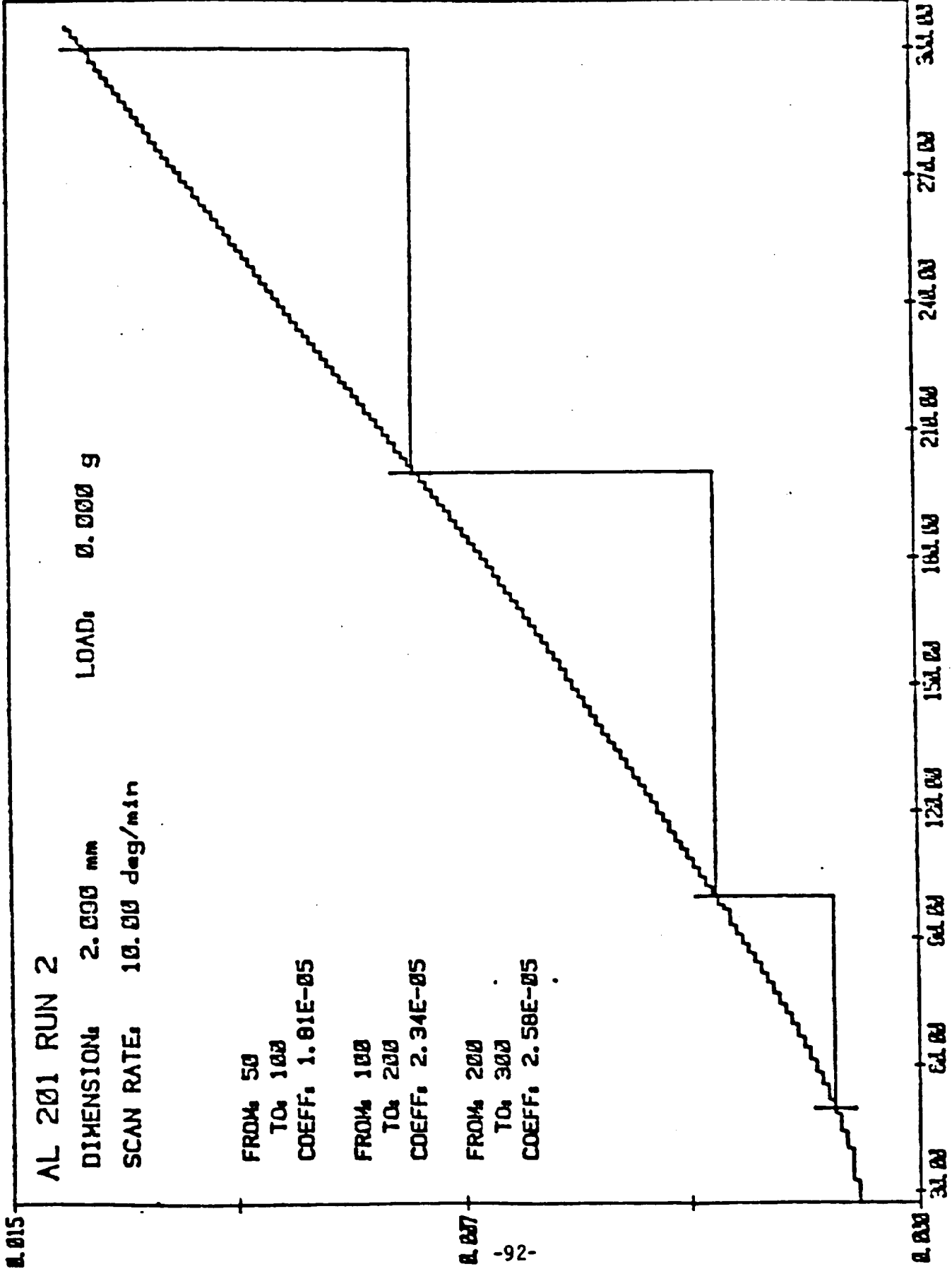
COMMENTS:

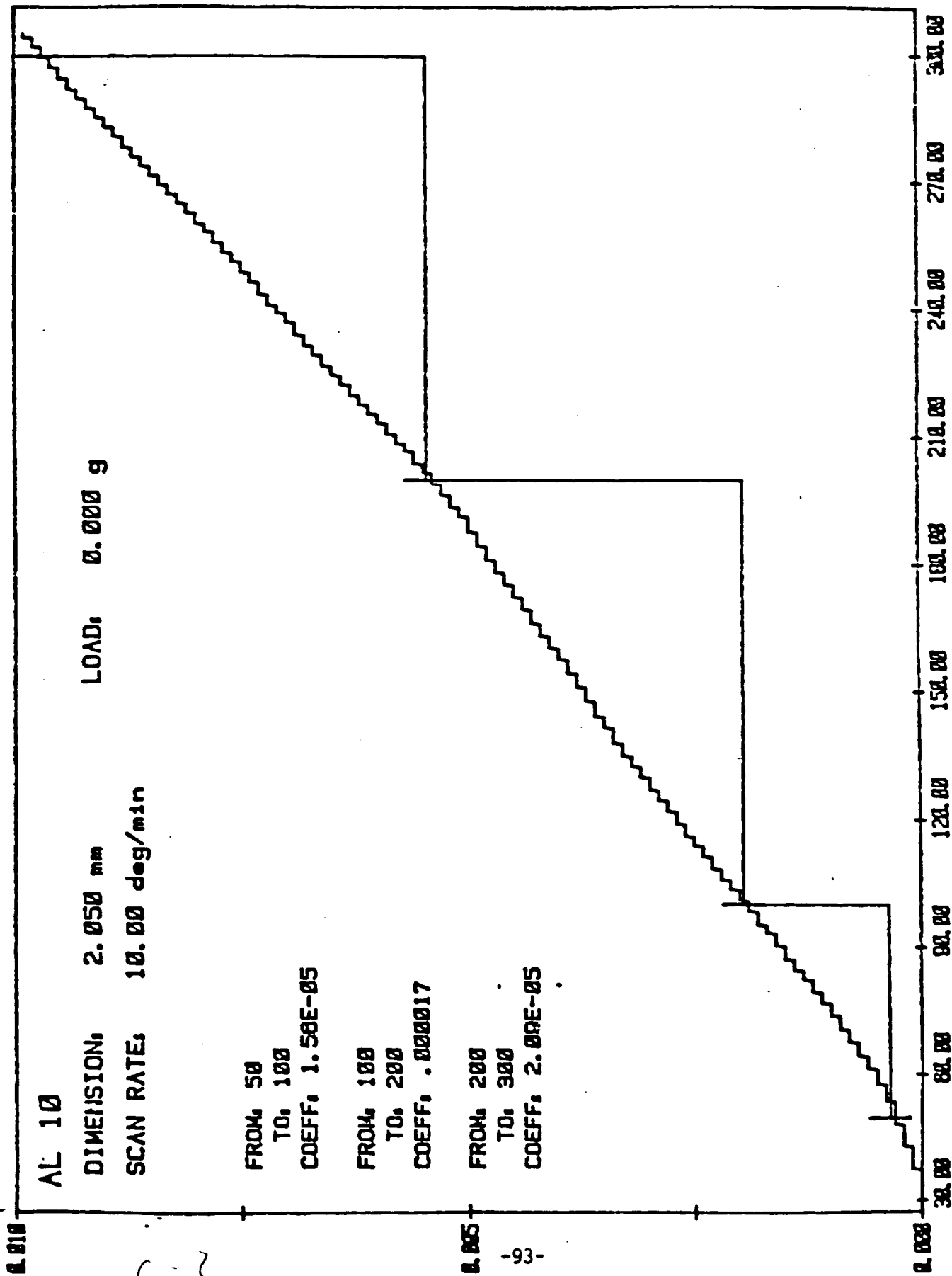
Original CTE measurements by strain gage monitoring were aborted when proper gages were not immediately available. Measurements recorded from improper gages yield erroneous data. The results of this report reflect measurements taken at Analytical Service Center in Irvine, California. These measurements were made under my direct supervision to expedite analysis.

Respectfully Submitted,



William Wirt,
Consultant





TM

TEMPERATURE (C)

FILE: AL10.TM

A. THOMAS

c-2

L. J. 15

AL 20

DIMENSION: 1.610 mm

LOAD: 0.000 g

SCAN RATE: 10.00 deg/min

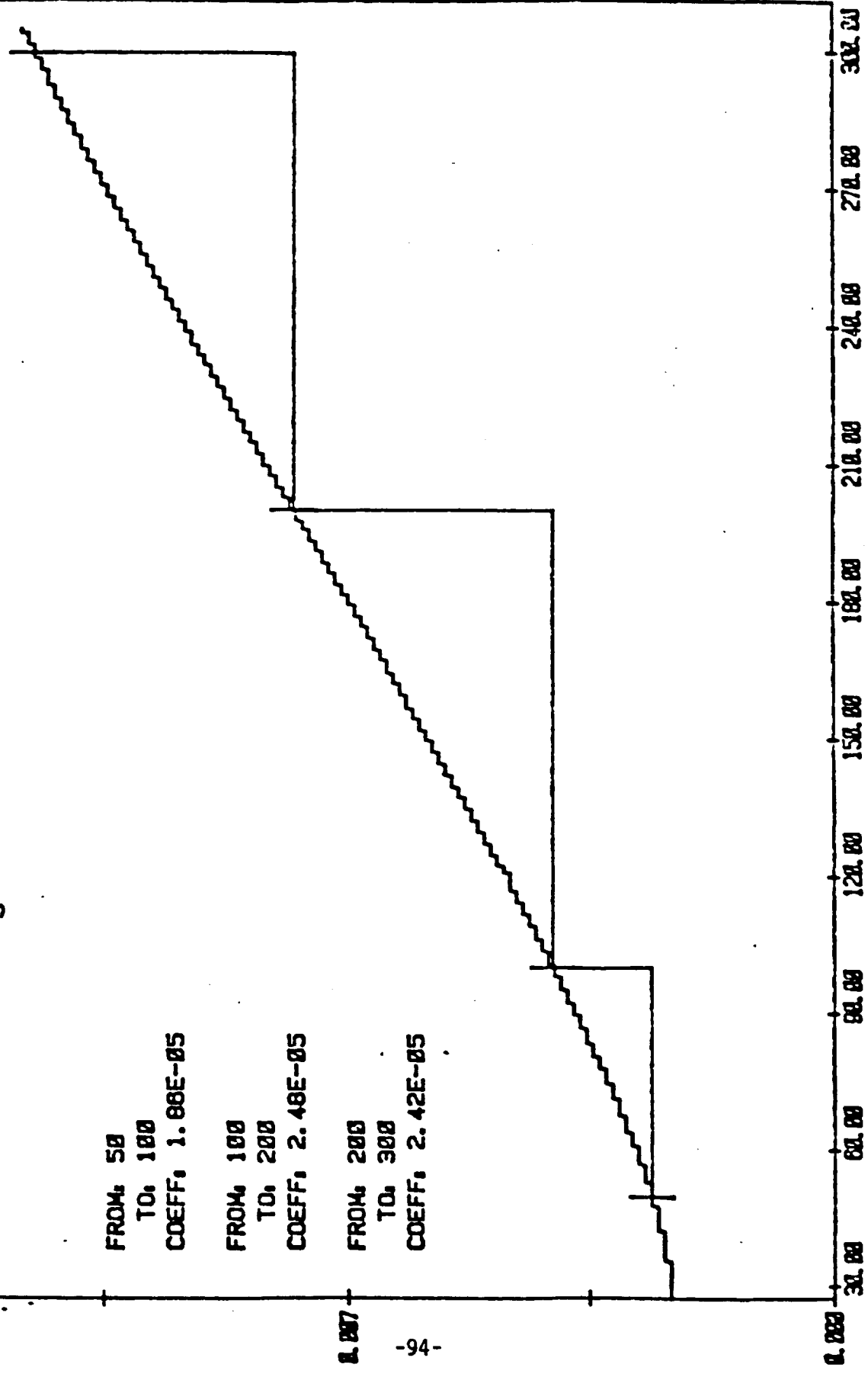
FROM: 50
TO: 100
COEFF: 1.88E-05

FROM: 100
TO: 200
COEFF: 2.48E-05

FROM: 200
TO: 300
COEFF: 2.42E-05

0.007

1.4



TMA

TEMPERATURE (C)

FILE: AL20.TM

A. THOMAS

...oys 200... cor opp...
 cipl alloying element, are very readily welda... and
 are particularly useful for elevated temperature appli-
 cations.

Specification	Product
AMS 4228	Castings (T6 temper)
AMS 4229	Castings (T7 temper)

3.12.1 201.0 ALLOY

3.12.1.0 *Comments and Properties.*—201.0 is a high-strength, heat-treatable Al-Cu-Ag casting alloy. It is very readily weldable. In the T6 (aged) temper, it possesses high strength and good ductility, but is not recommended for use in environments conducive to stress-corrosion cracking. In the T7 (overaged) temper, it possesses high strength and moderate ductility and optimum resistance to stress-corrosion cracking.

The temper index for 201.0 is as follows:

Section	Temper
3.12.1.1	T6
3.12.1.2	T7

3.12.1.1 *T6 Temper.*—A full-range tensile stress-strain curve for this temper is presented in Figure 3.12.1.1.6.

ORIGINAL PAGE IS
 OF POOR QUALITY

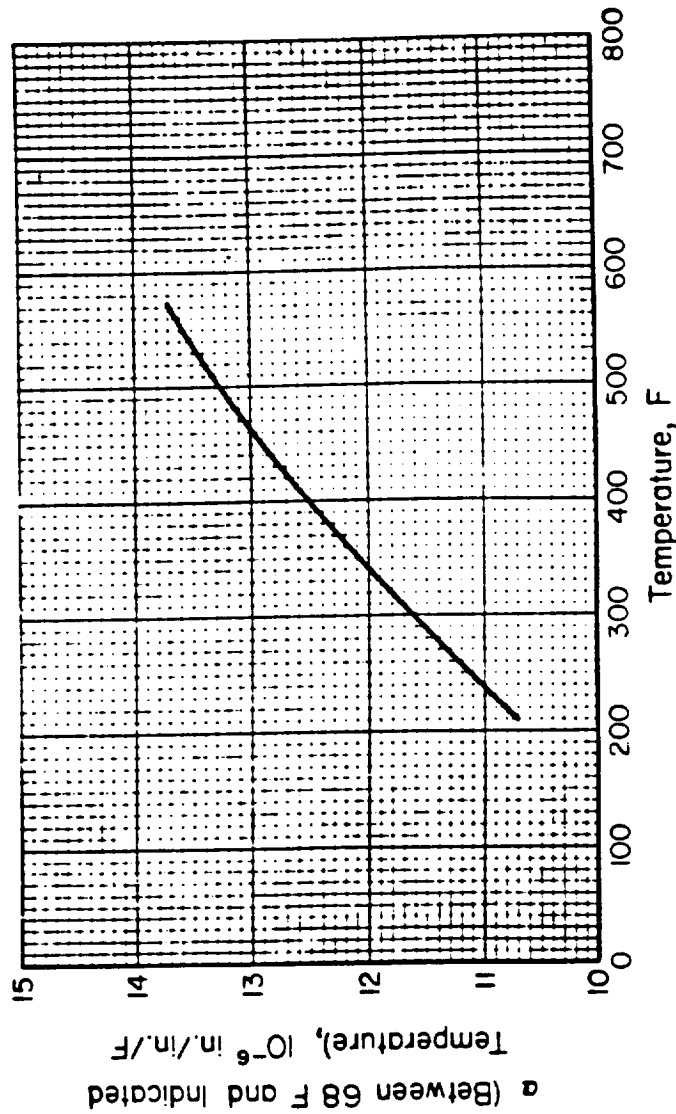
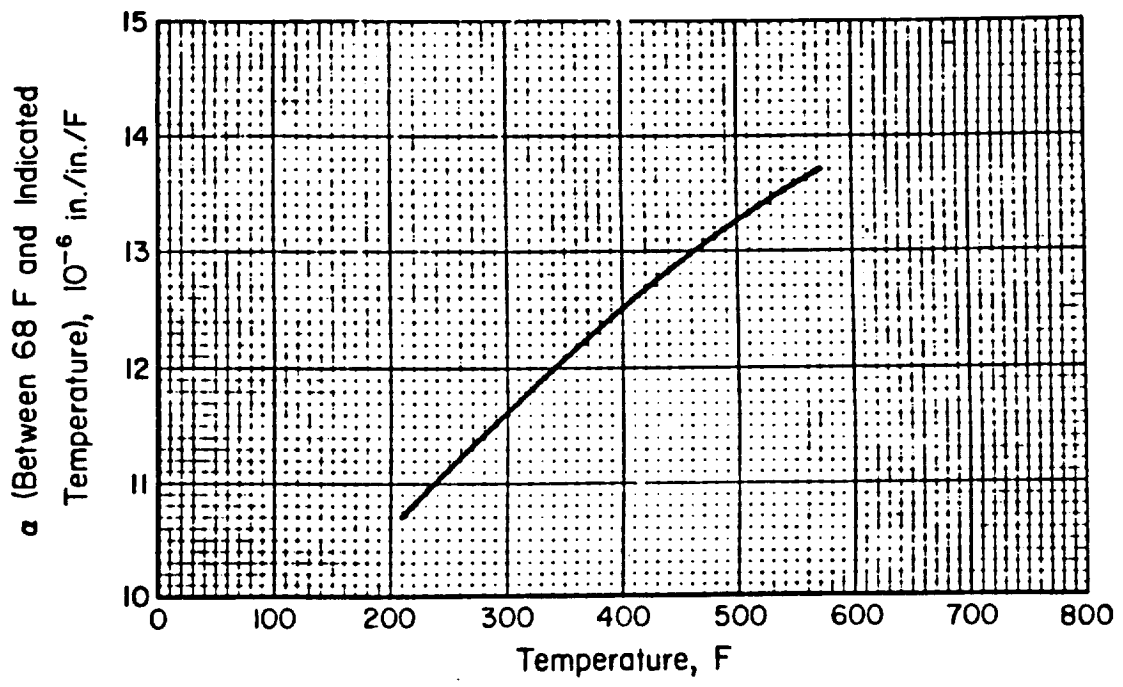


FIGURE 3.12.1.0. Effect of temperature on the physical properties of 201.0 aluminum alloy (castings).



Thermal Expansion of A201-T6
Metal Handbook Data